Electronic Supplementary Material (ESI) for Green Chemistry.

Supporting information

A rigid spirocyclic diol from fructose-based 5-hydroxymethylfurfural: Synthesis, life-cycle assessment, and polymerization for renewable polyesters and poly(urethane-urea)s

Niklas Warlin[1], Maria Nelly Garcia Gonzalez[2], Smita Mankar[1], Nitin Valsange[1], Mahmoud Sayed[3], Sang-Hyun Pyo[3], Nicola Rehnberg[1,4], Stefan Lundmark[5], Lars J. Nilsson[2], Rajni Hatti-Kaul[3], Patric Jannasch[1]*, Baozhong Zhang[1]**

1 Centre for Analysis and Synthesis, Department of Chemistry, Lund University, P.O. Box 124, SE-22100 Lund, Sweden.

2 Environmental and Energy Systems Studies, Lund University, Lund, Sweden.

3 Biotechnology, Department of Chemistry, Lund University, P.O. Box 124, SE-22100, Lund, Sweden.

4 Bona Sweden AB, Box 210 74, 200 21 Malmö, Sweden.

5 Perstorp AB, Innovation, Perstorp Industrial Park, 284 80 Perstorp, Sweden.

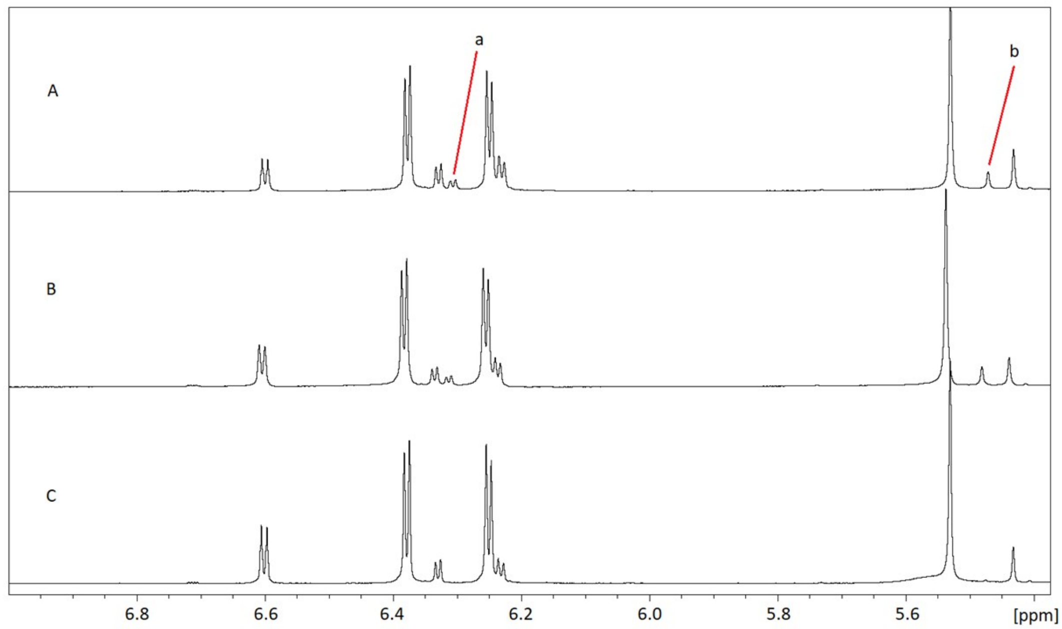

Figure S1. ^{1}H NMR spectra of the crude reaction mixture of the monomer synthesis, using (A) EtOH, (B) PrOH, and (C) 2-PrOH as the solvents. The marked signals (a and b) were due to side reactions, which were not observed in (C).

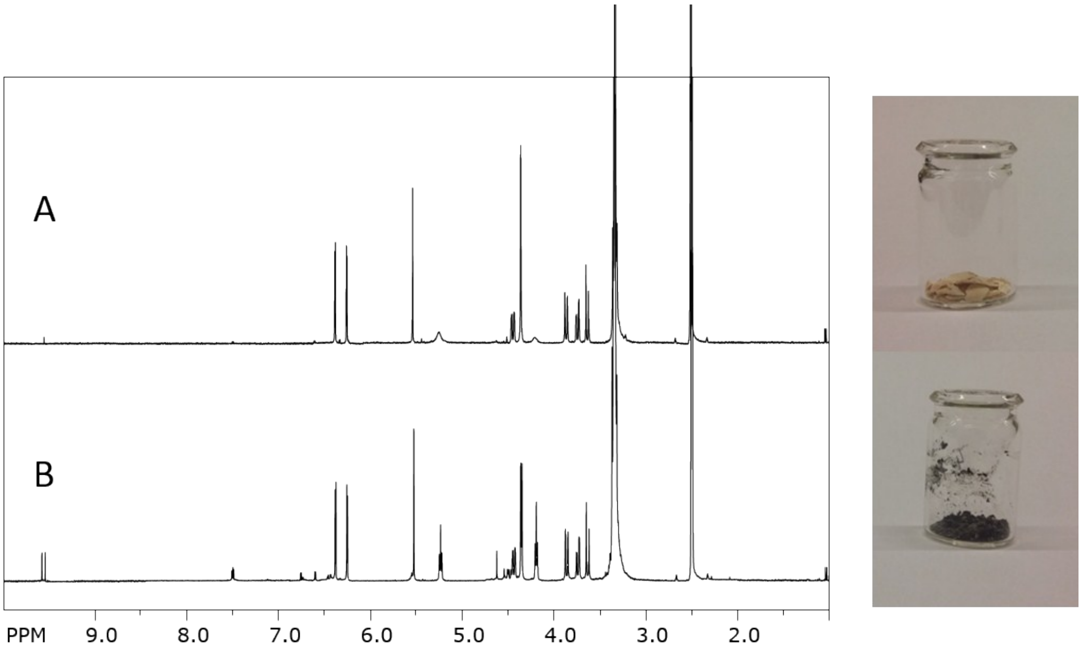

Figure S2. ^{1}H NMR spectra of the crude reaction mixture after (A) being quenched with $NaHCO_3$ and vacuum-dried, and (B) vacuum-dried without base-quenching.

Monomer synthesis using fructose-based HMF

Fructose-based HMF was synthesized by dehydration of fructose in DMSO. Visual inspection of the samples showed that the fructose-based HMF showed a darker colour than the commercial HMF (Fig. S23). According to ^{1}H NMR spectroscopical analyses (Fig. S24), the fructose-based HMF contained small amount of impurities (marked by red arrows). Furthermore, LC-MS results revealed that the purity of the fructose-based HMF 88%, while the purity for the commercial HMF was >95%. Finally, the fructose-based HMF was subjected to the synthesis of Monomer **S** according to the optimized experimental procedure. After the reaction, the crude reaction mixture was dried and subjected to ^{1}H NMR analyses (Fig. S25). The conversion of HMF was calculated according to the NMR integrals (Fig. S25). As a result, the HMF conversion by using fructose-based HMF was ~70%, which was slightly lower than the conversion for the monomer synthesis using commercial HMF-C (~75%).

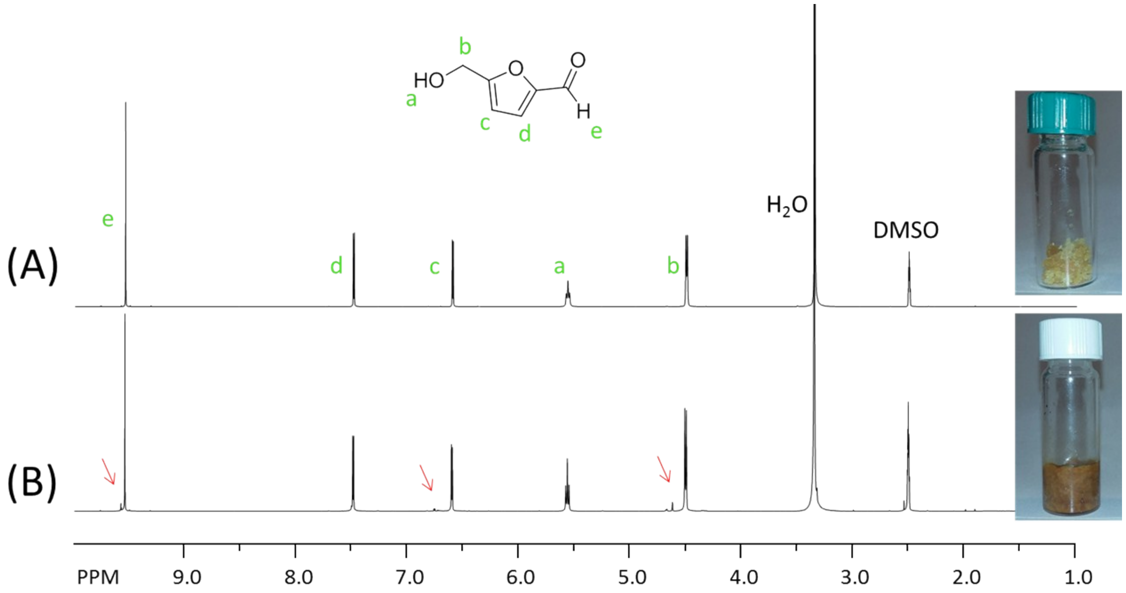

Figure S3. ^{1}H NMR-spectra of (A) commercial HMF and (B) fructose-based HMF. The red arrows pointed at some minor impurity peaks in (B).

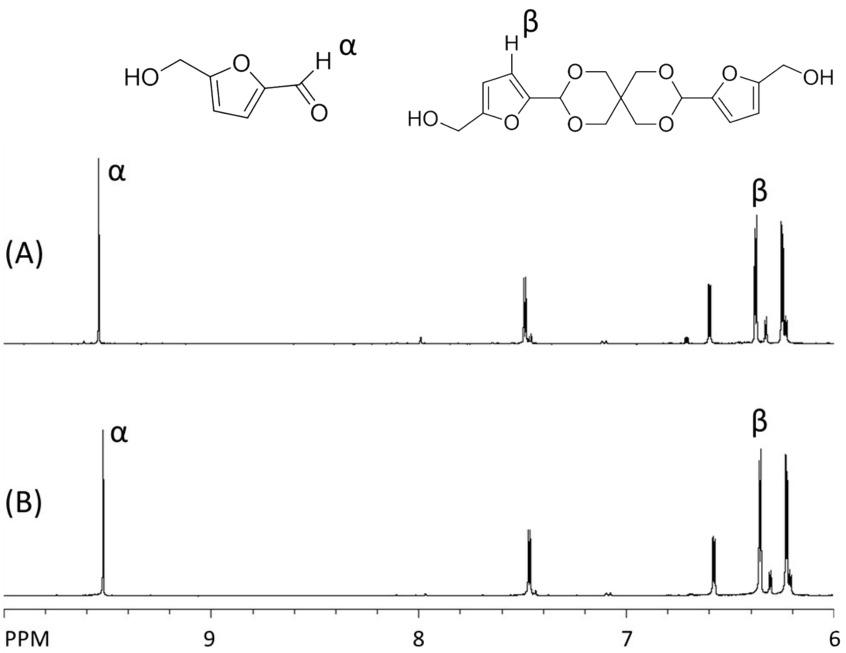

Figure S4. ^{1}H NMR-spectra of the crude reaction mixture using (A) commercial HMF and (B) fructose-based HMF. The conversion was calculated according to the integrals of the aldehyde proton of HMF (α) and the furan proton of Monomer **S** (β).

Figure S5. PHST-19 synthesized (A) with the solvents (xylene and mesitylene) under nitrogen, and (B) under vacuum condition without solvent.

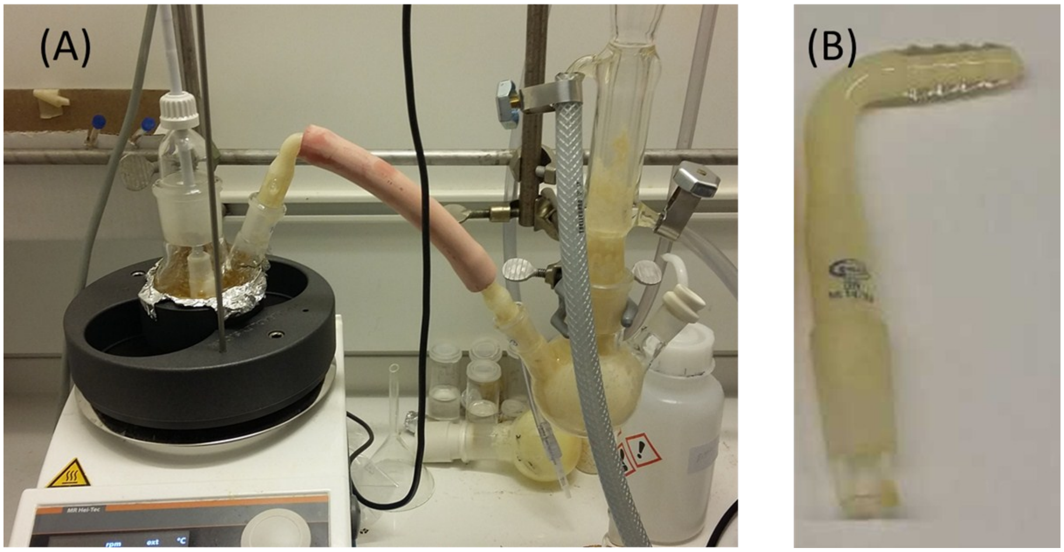

Figure S6. (A) Polymerization of PHST-19 with antioxidant TNPP under vacuum condition. (B) the vacuum outlet blocked by the foams formed in the polymerization.

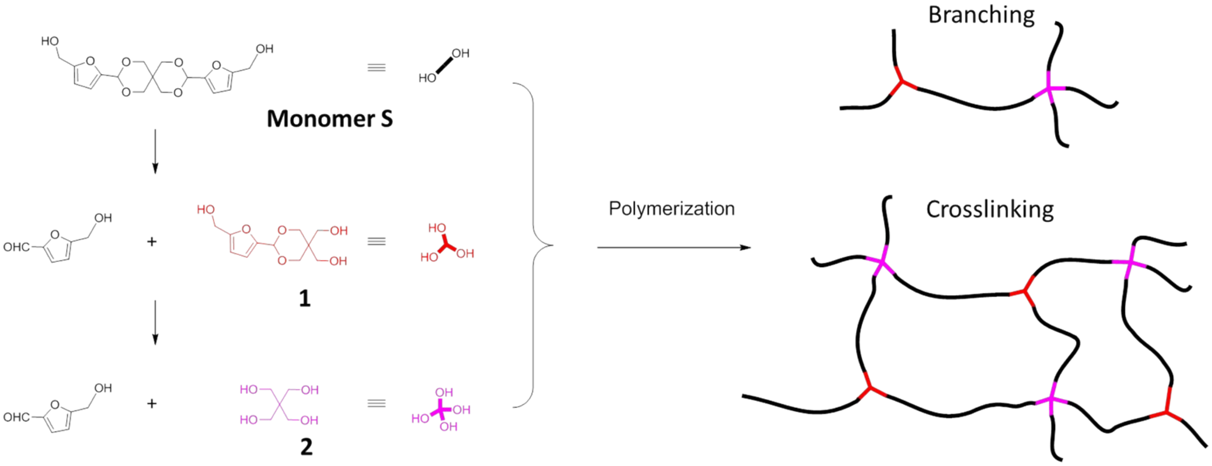

Figure S7. Possible thermal degradation of Monomer S to form HMF and polyols, leading to subsequent branching or crosslinking.

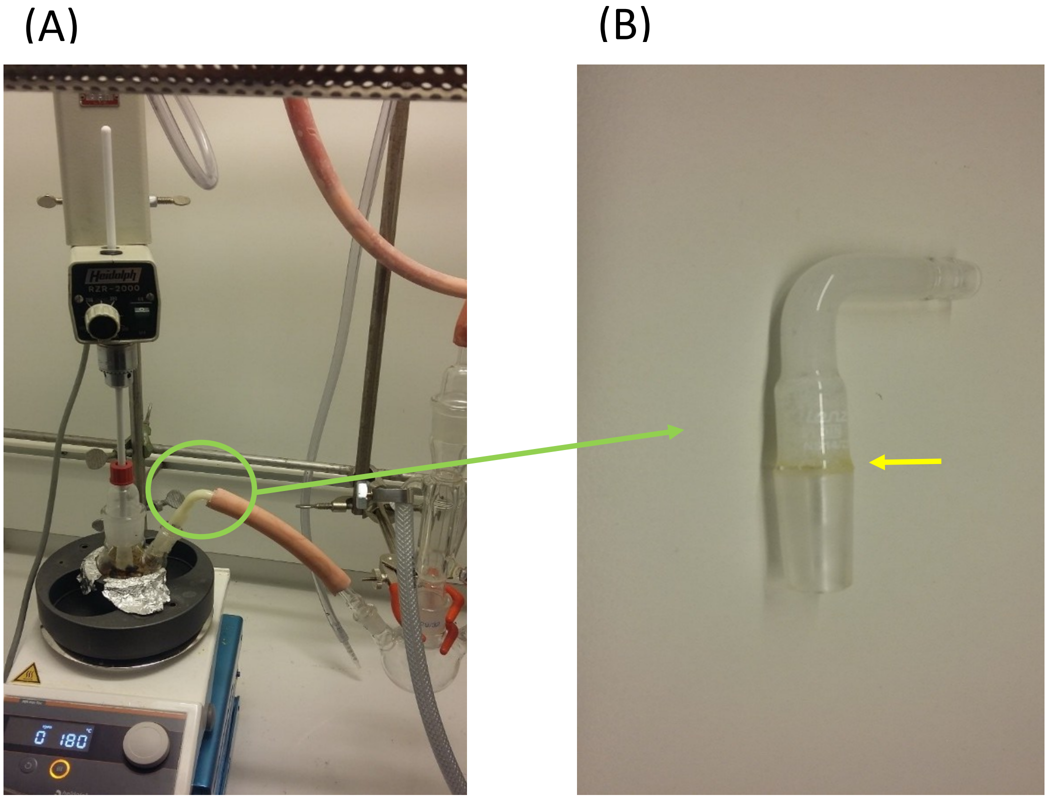

Figure S8. (A) An on-going polycondensation reaction with the vacuum outlet highlighted by the green circle, (B) the vacuum outlet after the polycondensation. The yellow arrow pointed at the yellow solid formed inside the vacuum outlet, which was collected and measured by ^{1}H NMR analysis (Figure S4).

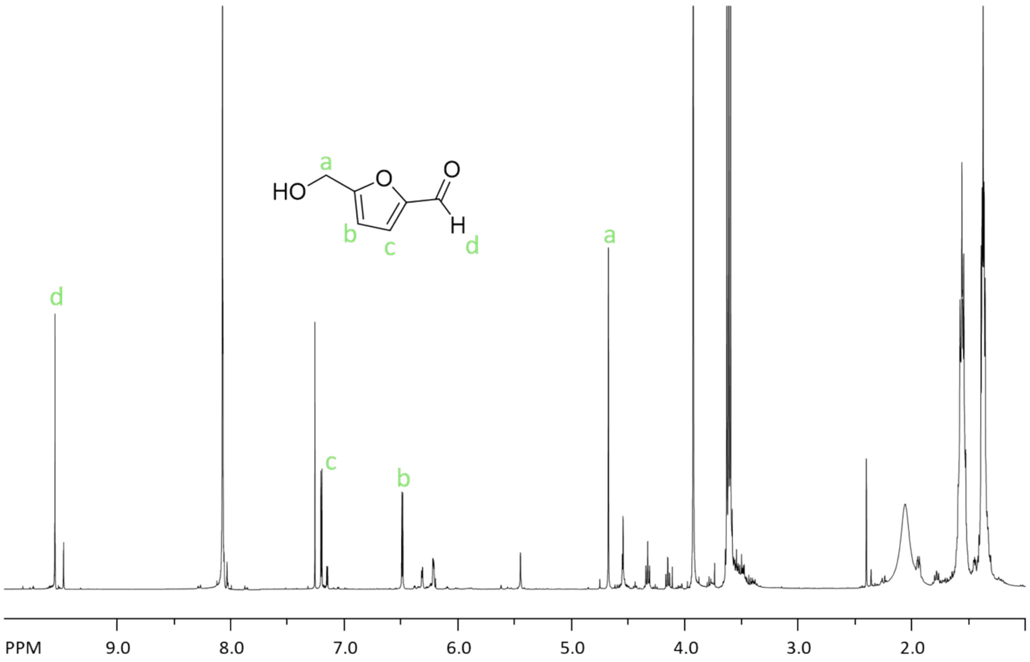

Figure S9. ^{1}H NMR-spectrum of the yellow solid collected from vacuum outlet after the polymerization.

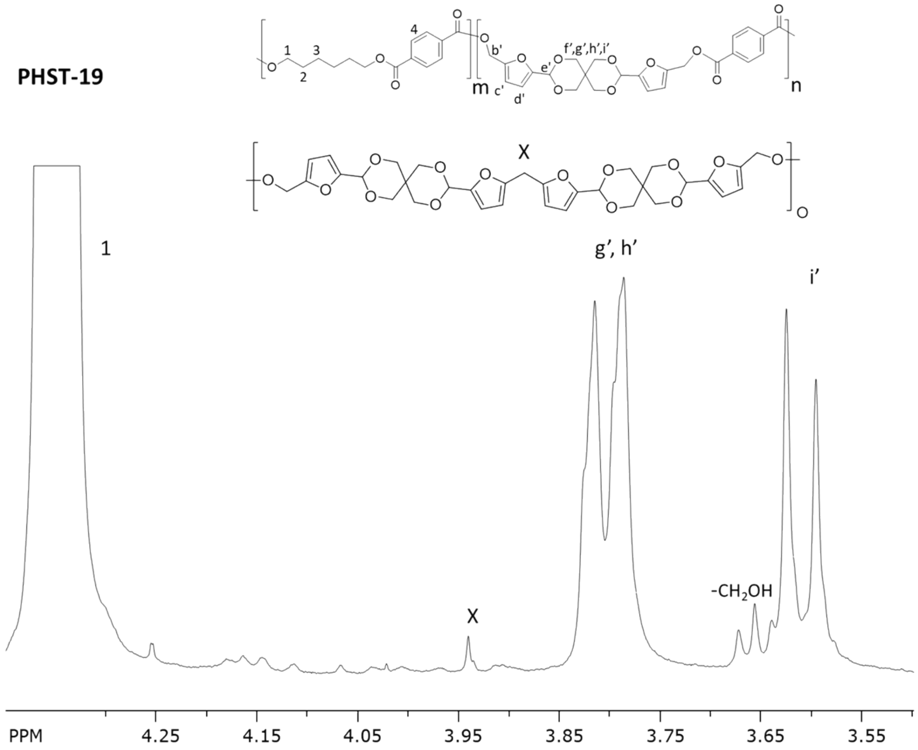

Figure S10. ^{1}H NMR spectrum of PHST-18 (expanded from 5.0 to 3.0 ppm)

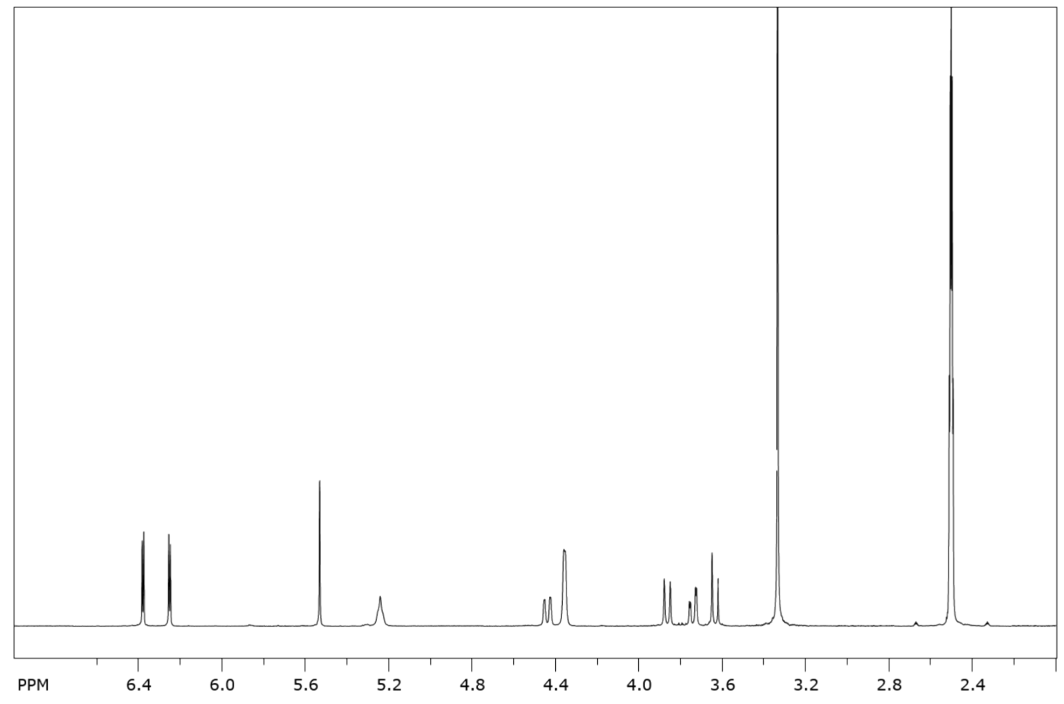

Figure S11. ^{1}H NMR spectrum of Monomer **S**.

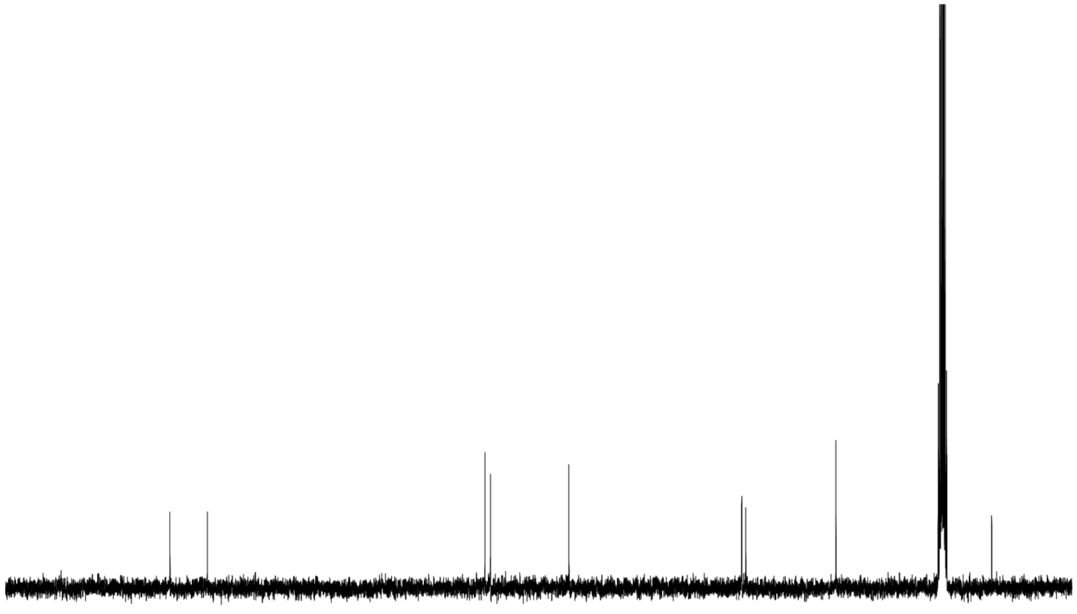

Figure S12. ^{13}C NMR spectrum of Monomer **S**.

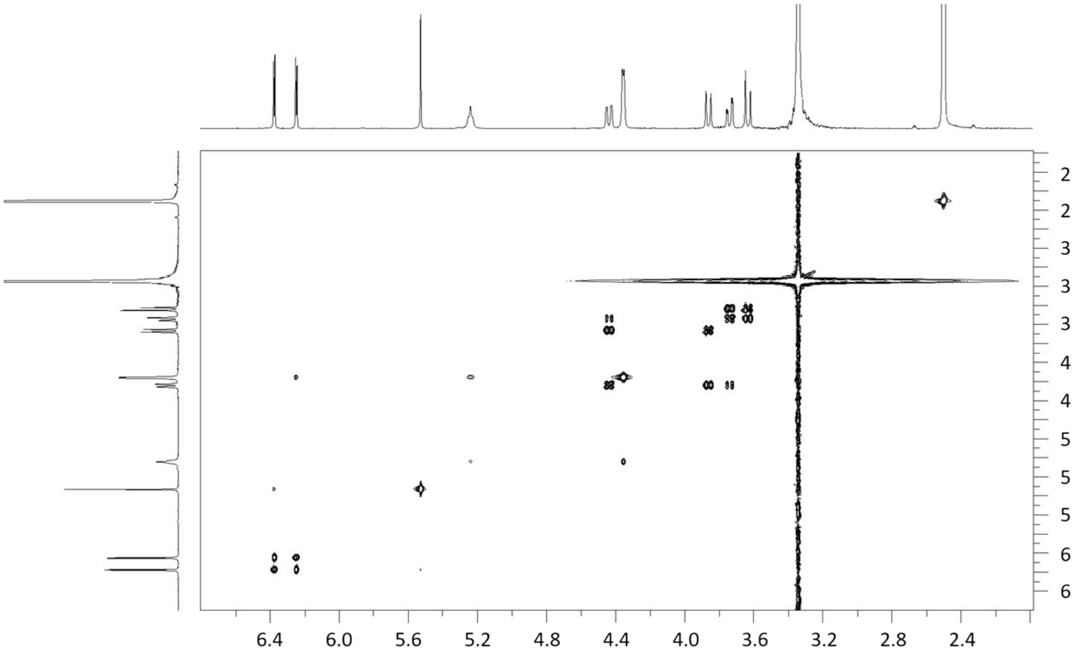

Figure S13. COSY spectrum of Monomer **S**.

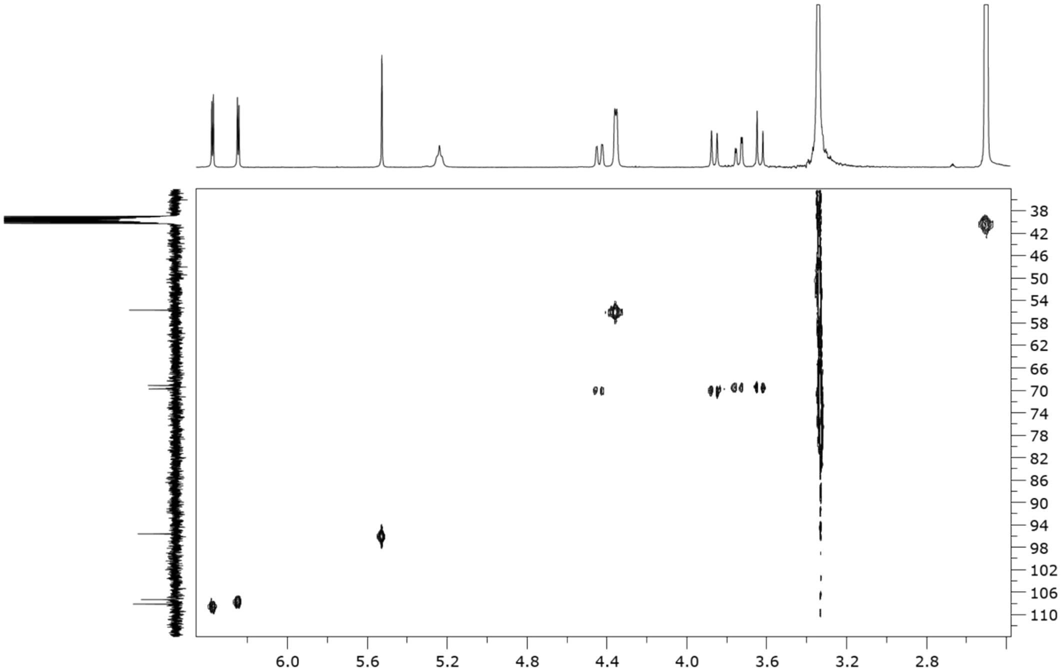

Figure S14. HMQC spectrum of Monomer **S**.

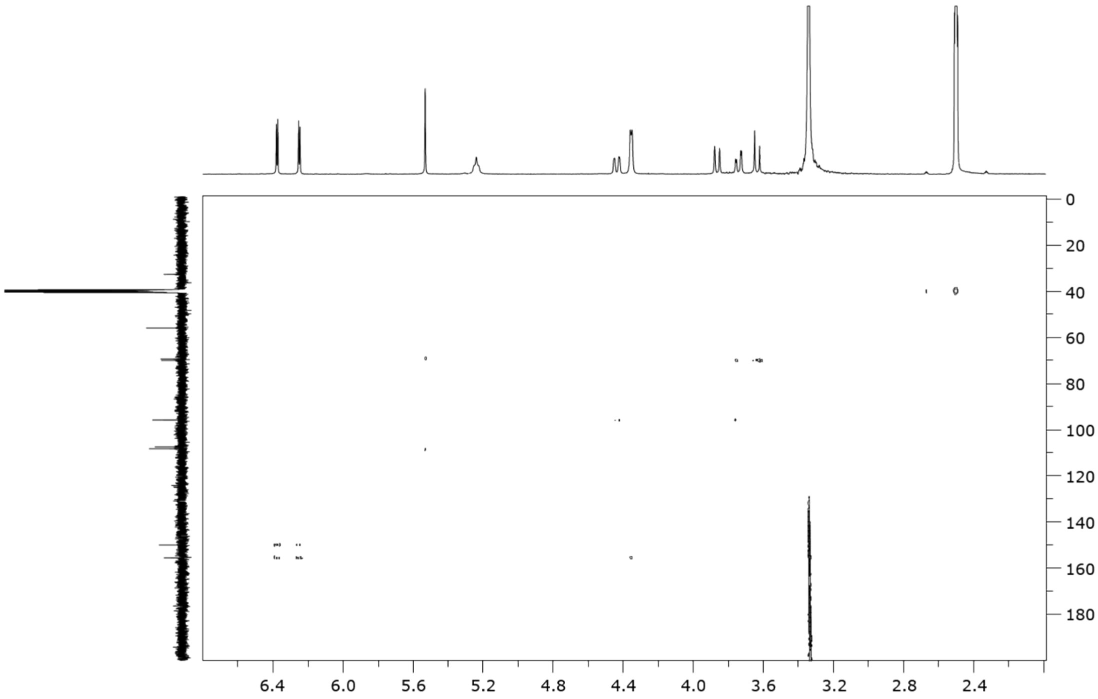

Figure S15. HMBC spectrum of Monomer **S**.

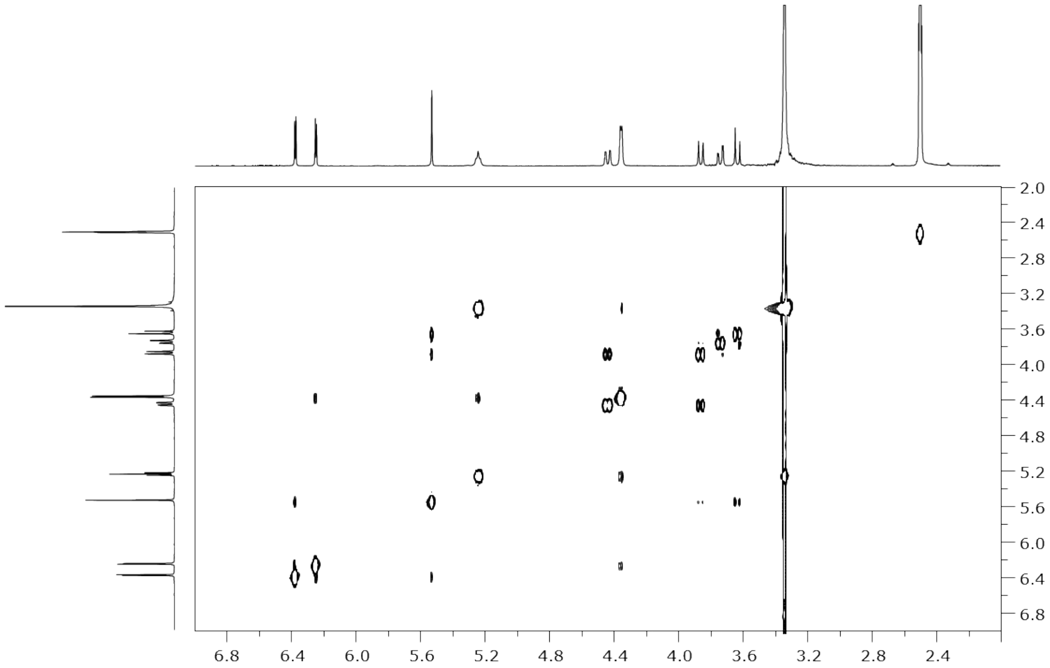

Figure S16. NOESY spectrum of Monomer **S**.

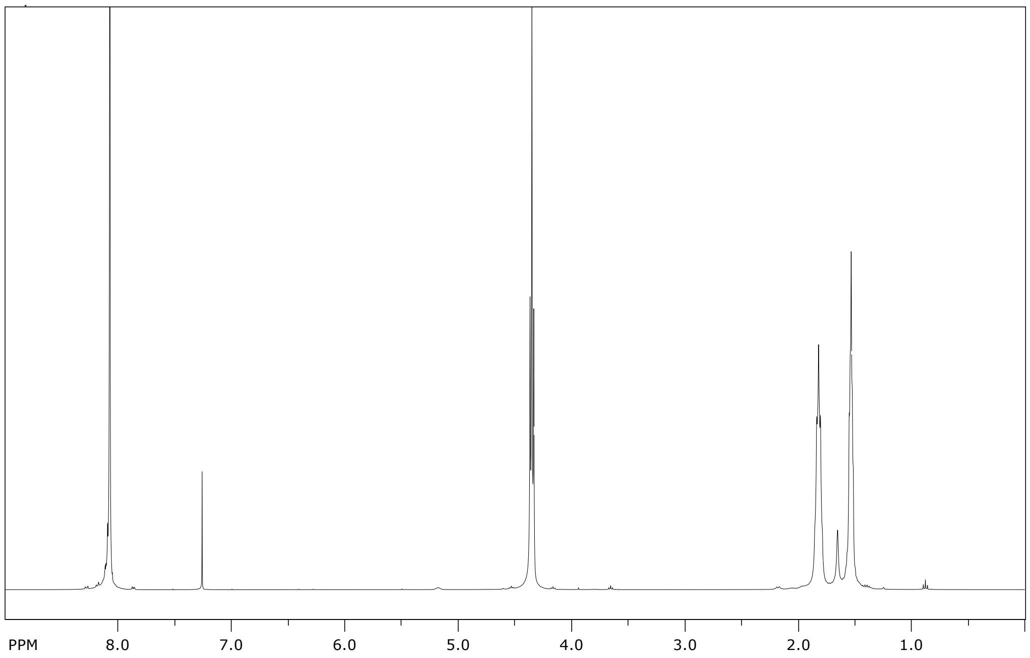

Figure S17. ^{1}H NMR spectrum of PHT.

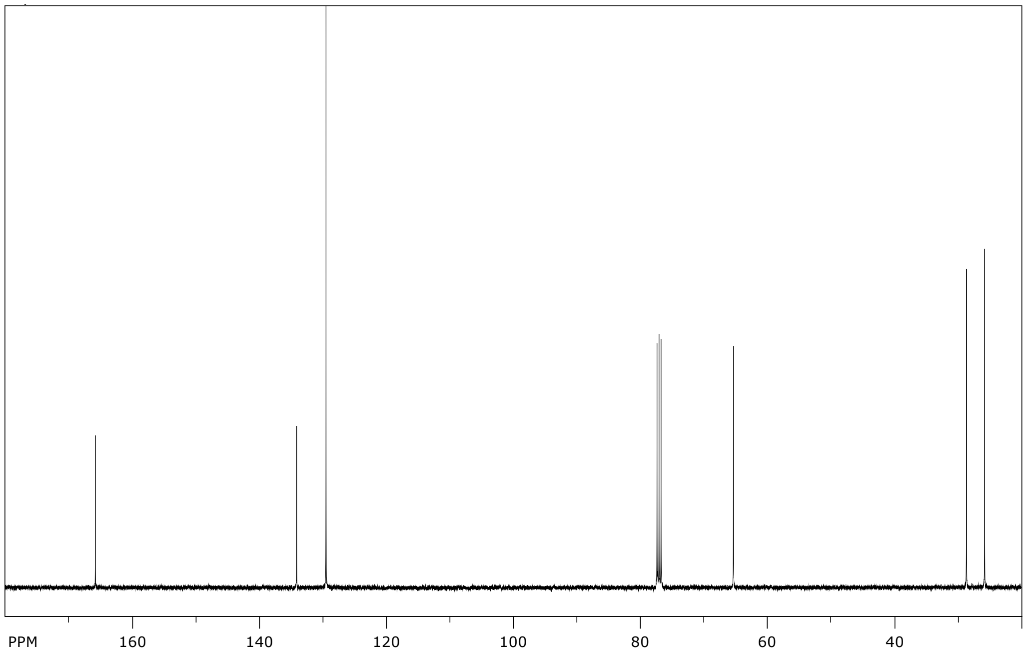

Figure S18. ^{13}C NMR spectrum of PHT.

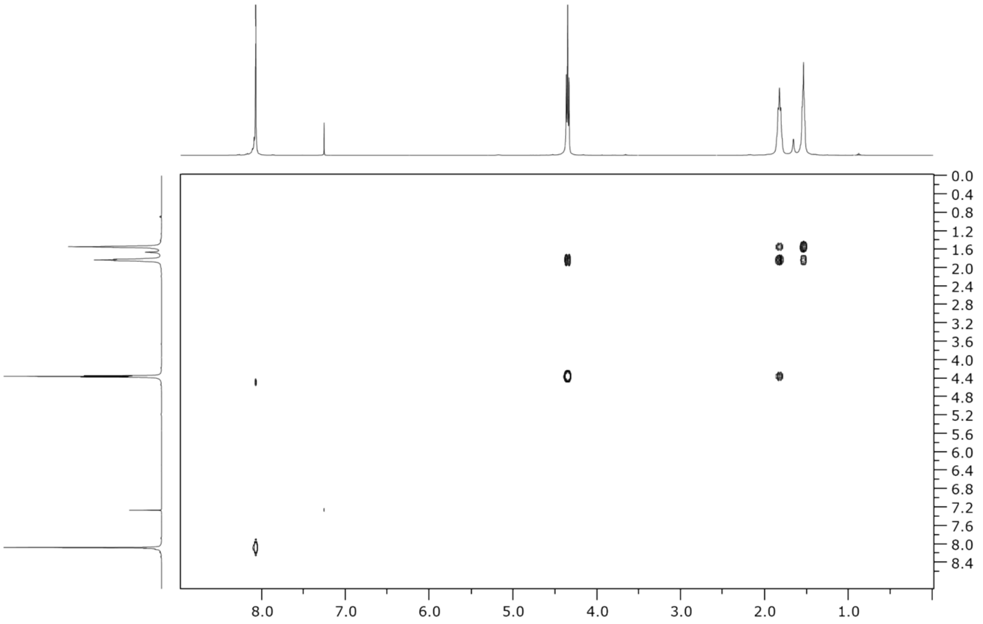

Figure S19. COSY spectrum of PHT.

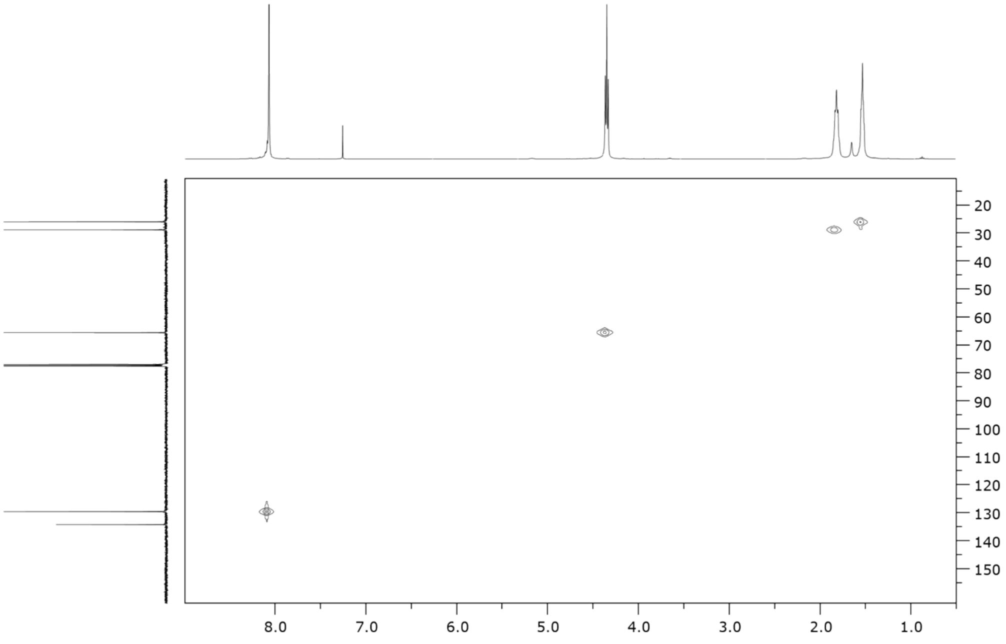

Figure S20. HMQC spectrum of PHT.

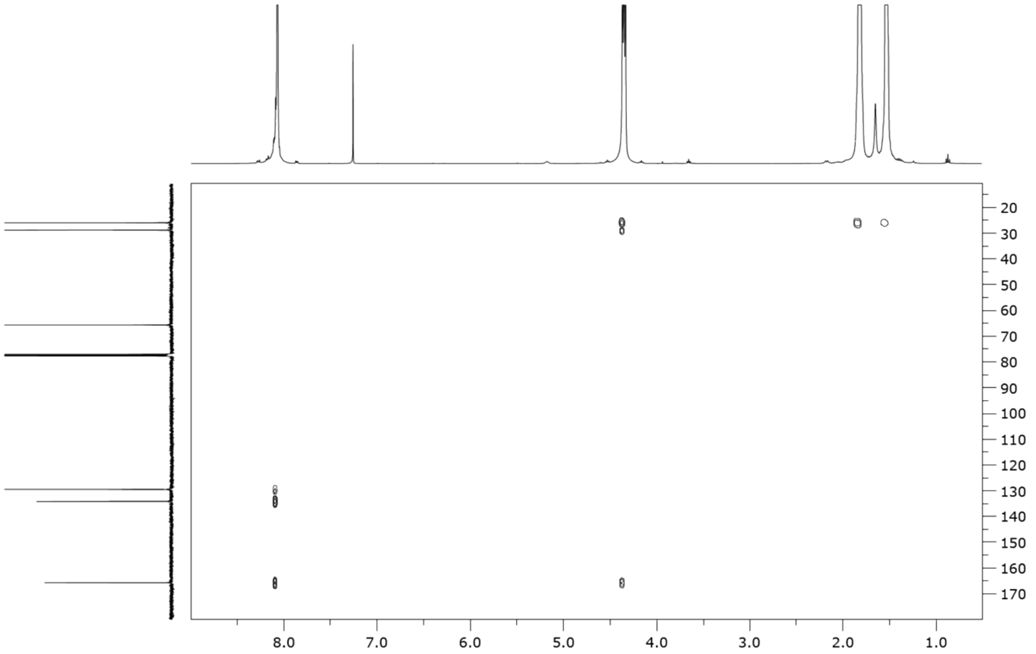

Figure S21. HMBC spectrum of PHT.

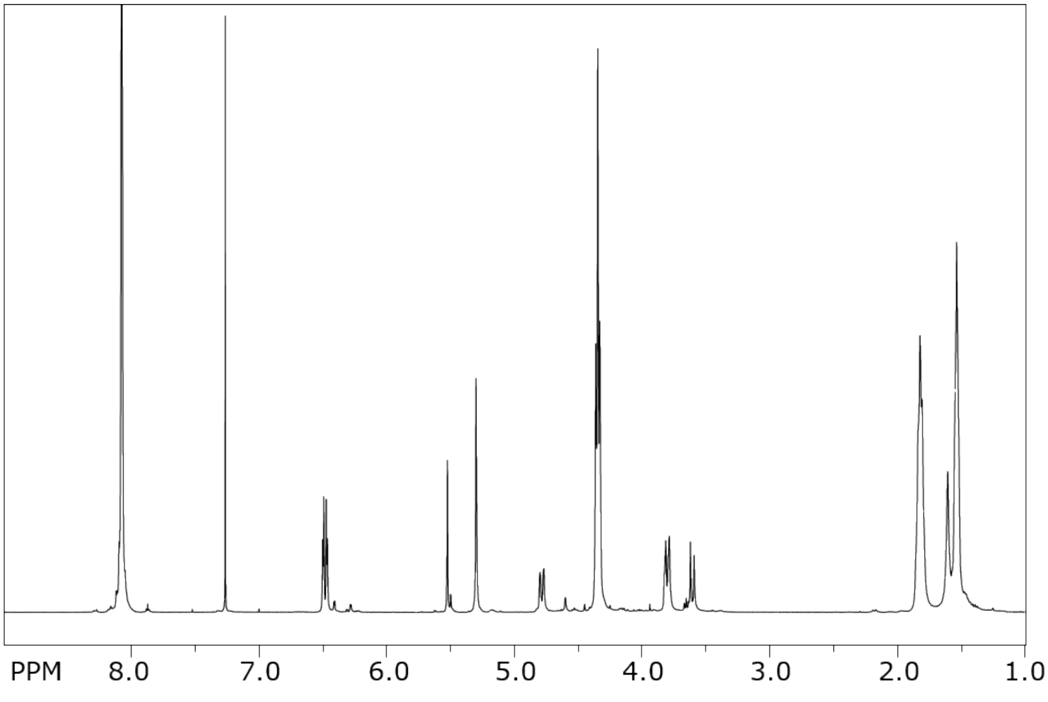

Figure S22. ^{1}H NMR spectrum of PHST-19.

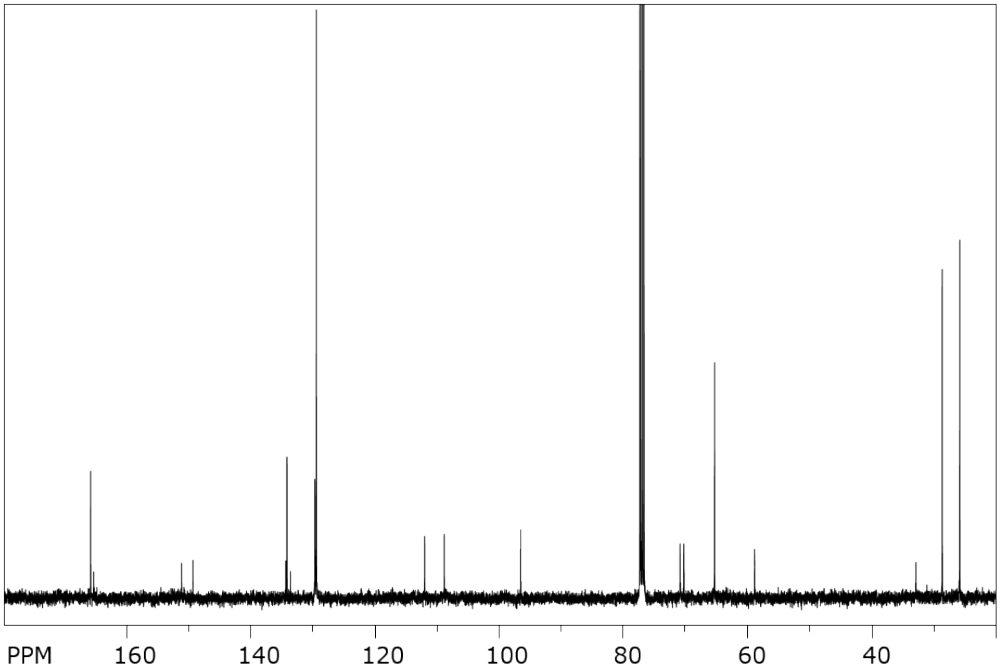

Figure S23. ^{13}C NMR spectrum of PHST-19.

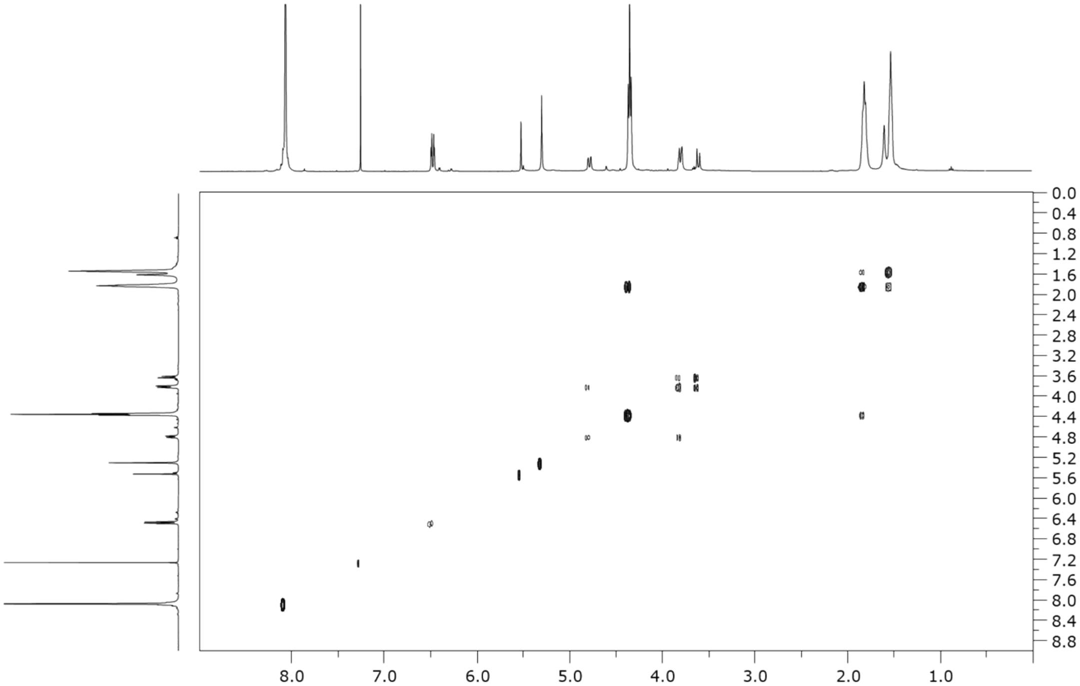

Figure S24. COSY spectrum of PHST-19.

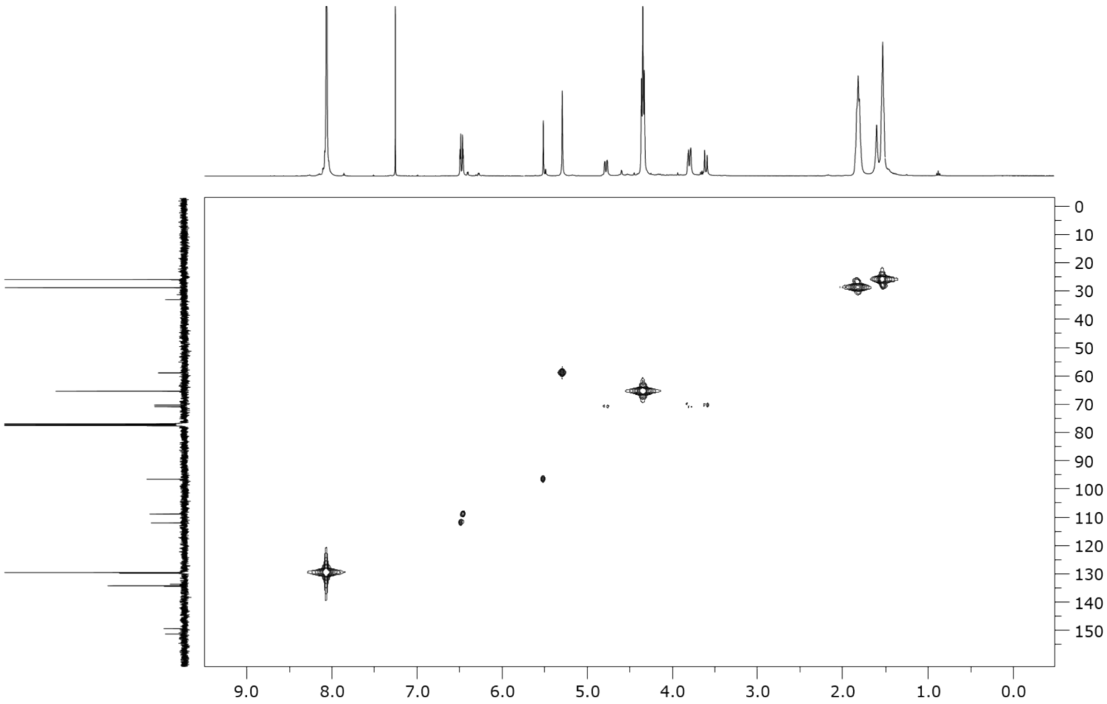

Figure S25. HMQC spectrum of PHST-19.

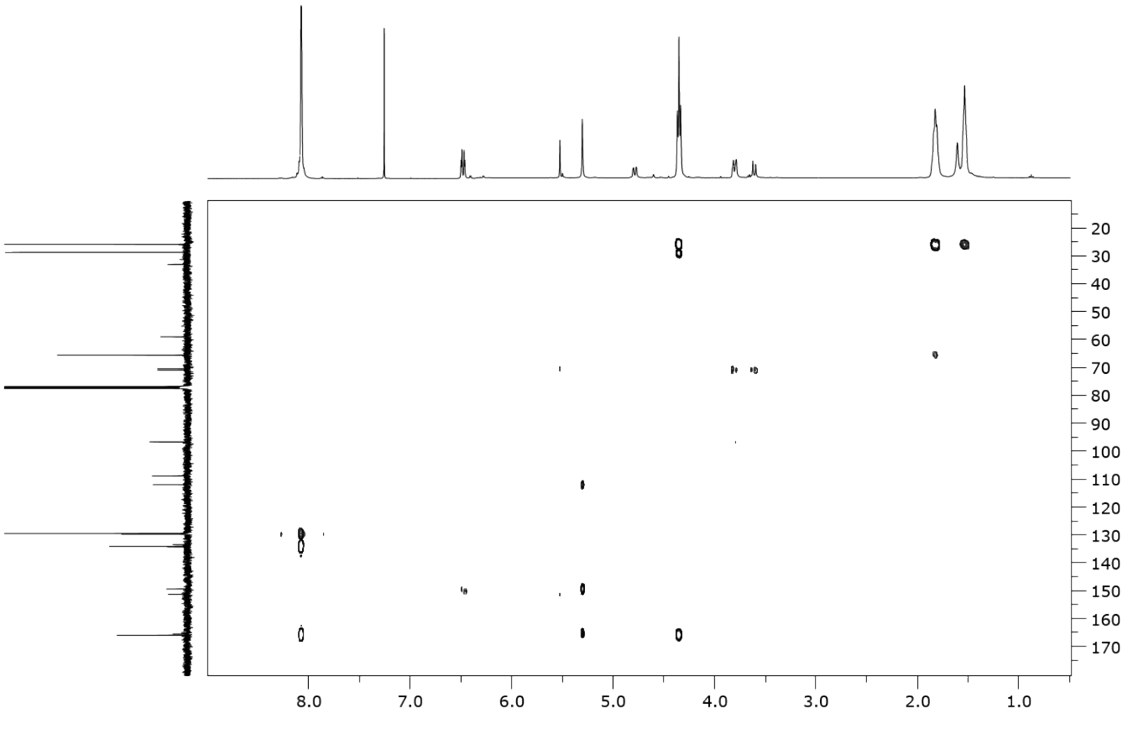

Figure S26. HMBC spectrum of PHST-19.

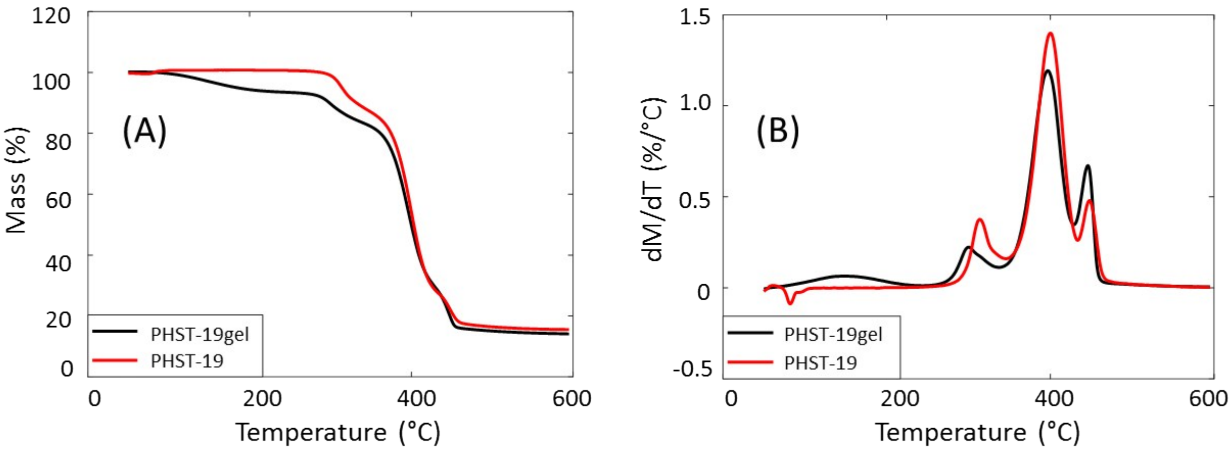

Figure S27. (A) TGA thermograms, and (B) derivative curves of PHST-19gel and PHST-19.

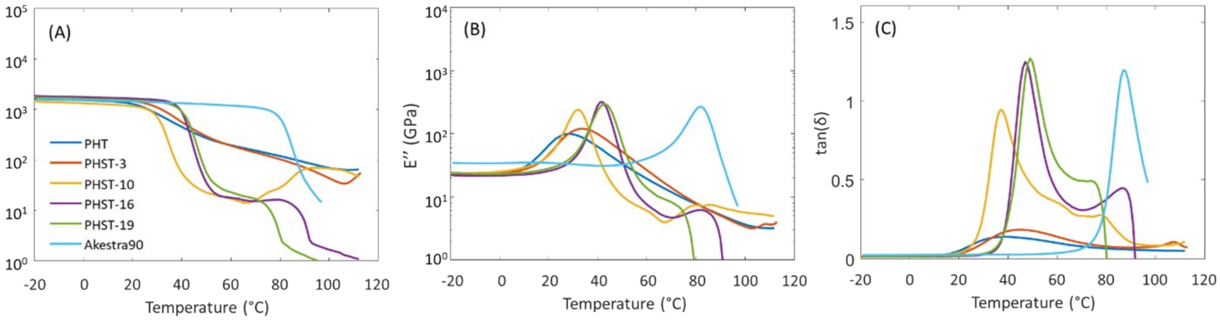

Figure S28. DMA results, including the (A) storage modulus, (B) loss modulus and (C) tan δ for the synthesized (PHT and PHSTs) and a commercial polyester (Akestra 90).

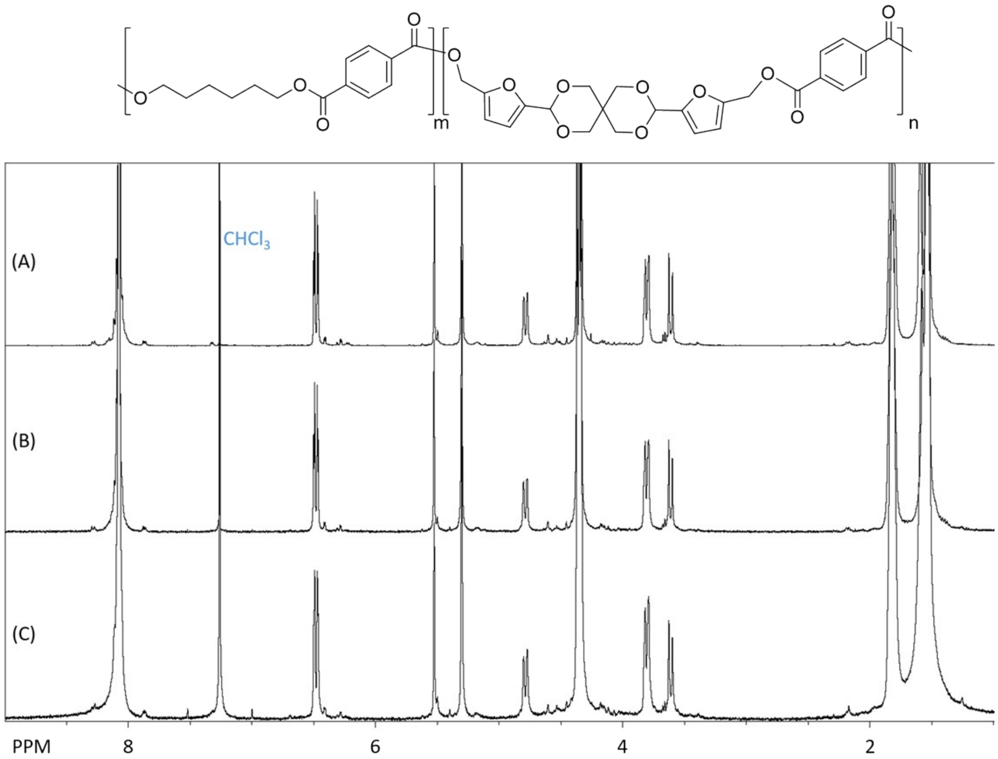

Figure S29. Blow-up of the ^{1}H NMR spectra of PHST-16. (A) Before rheological measurement, (B) after time-sweep rheology measurement 170 °C, and (C) after time-sweep rheology measurement at 200 °C.

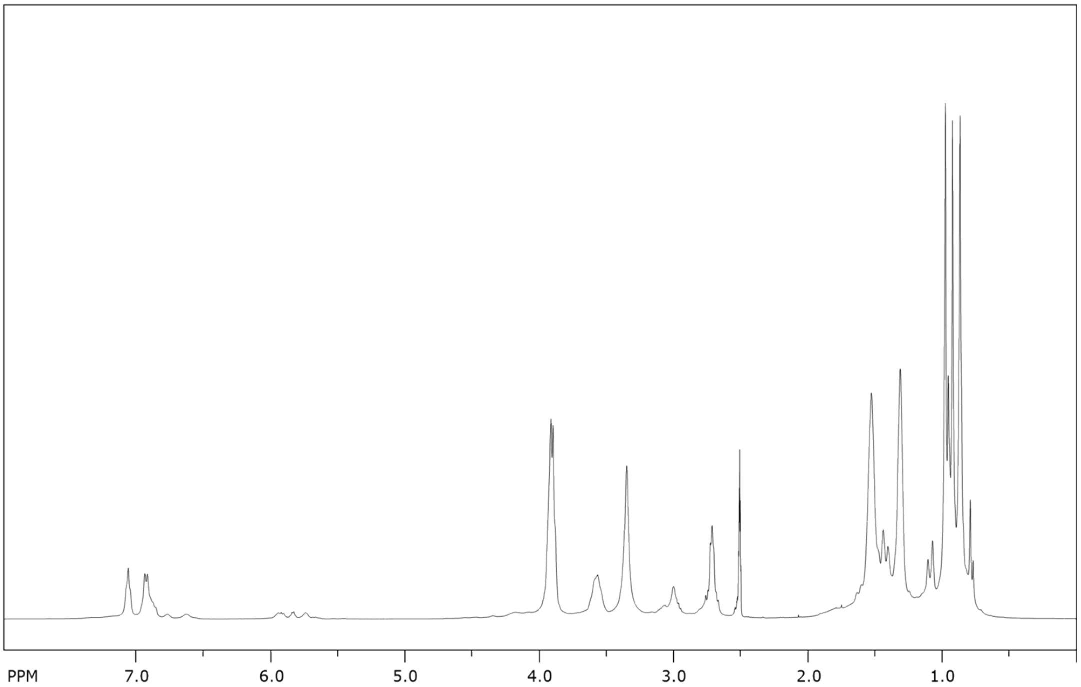

Figure S30. ^{1}H NMR spectrum of PU.

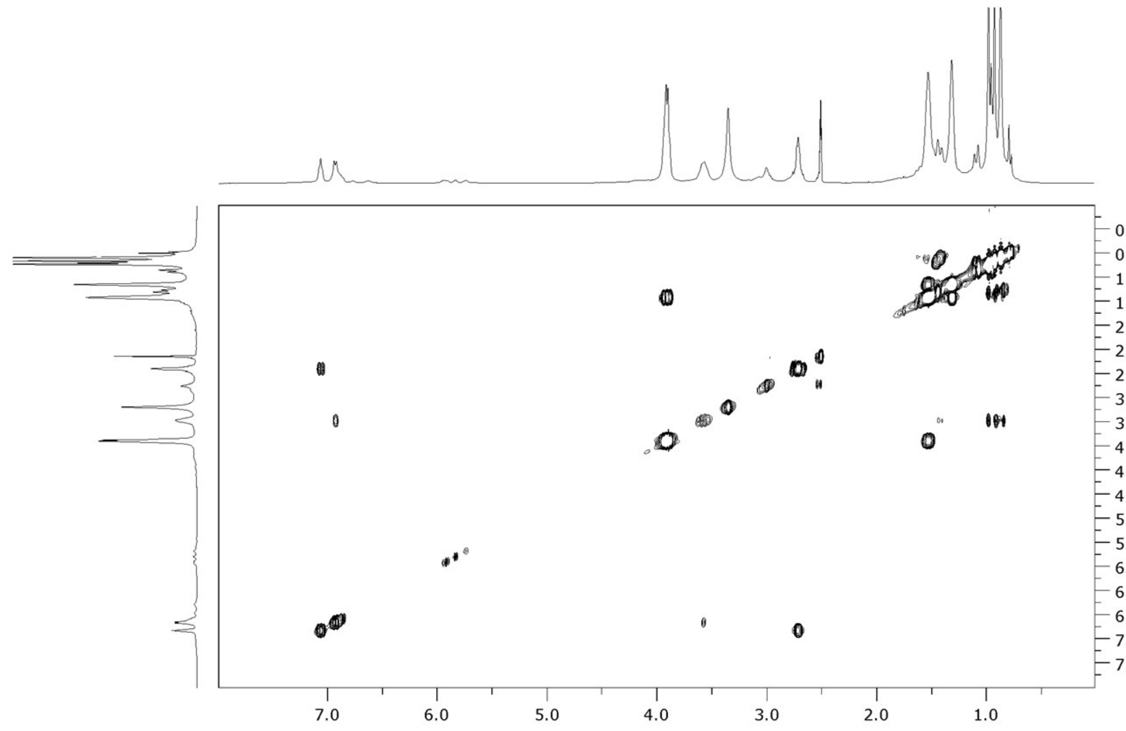

Figure S31. COSY spectrum of PU.

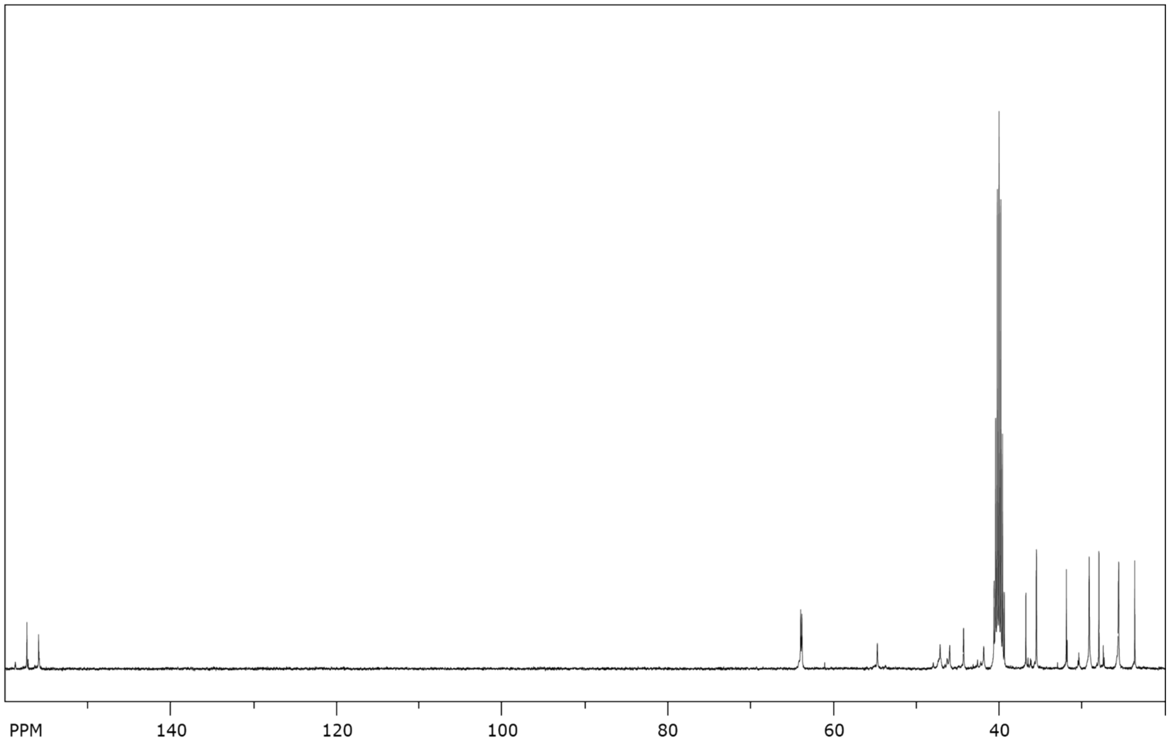

Figure S32. ^{13}C NMR spectrum of PU.

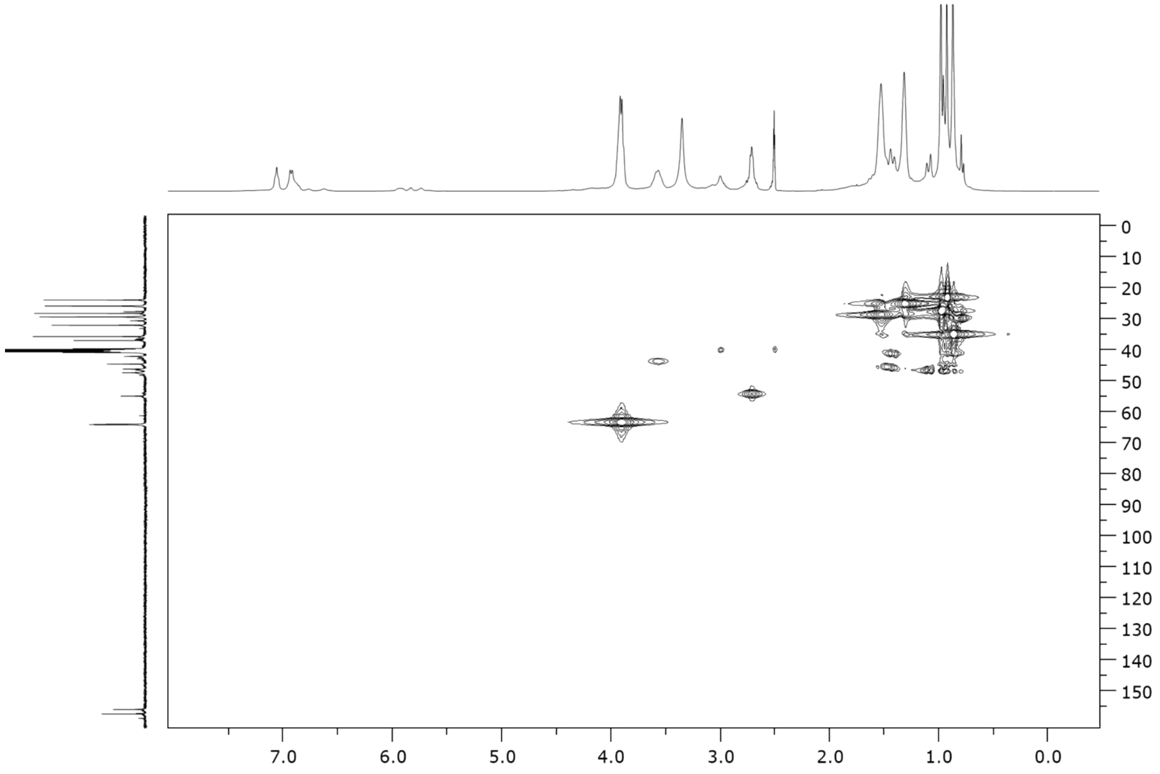

Figure S33. HMQC spectrum of PU.

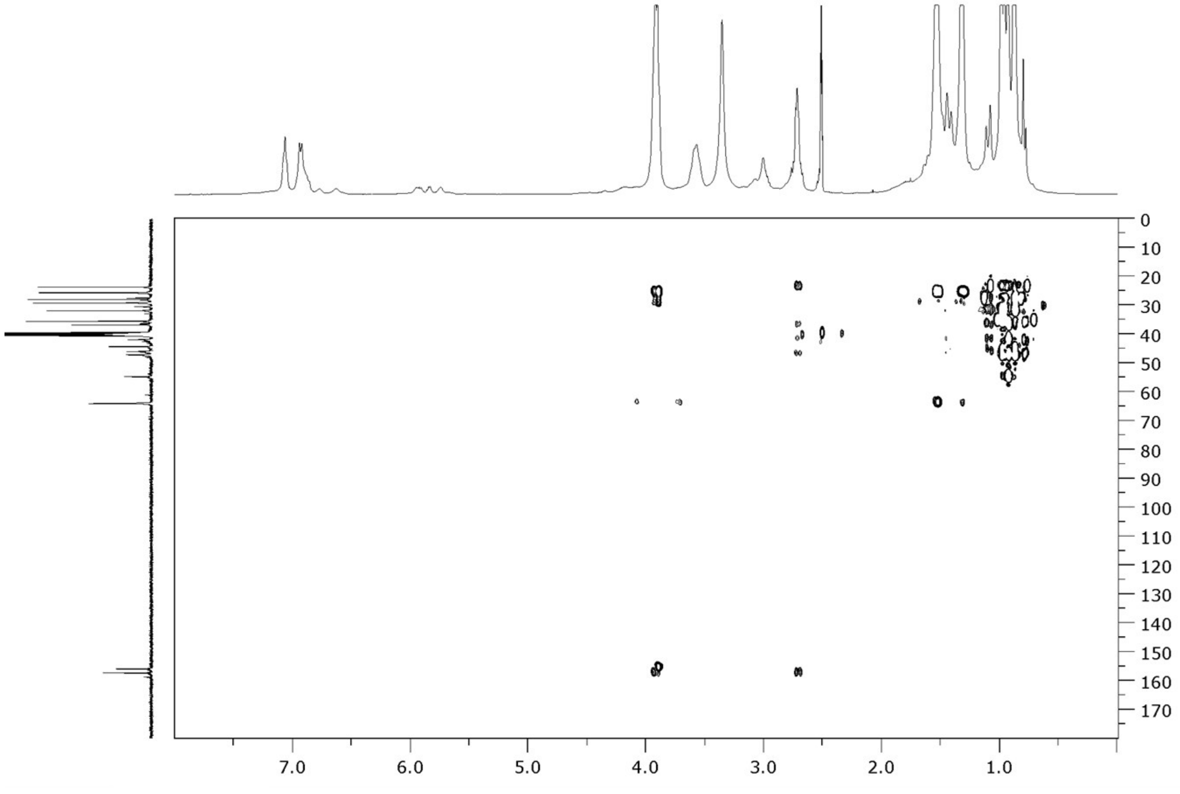

Figure S34. HMBC spectrum of PU.

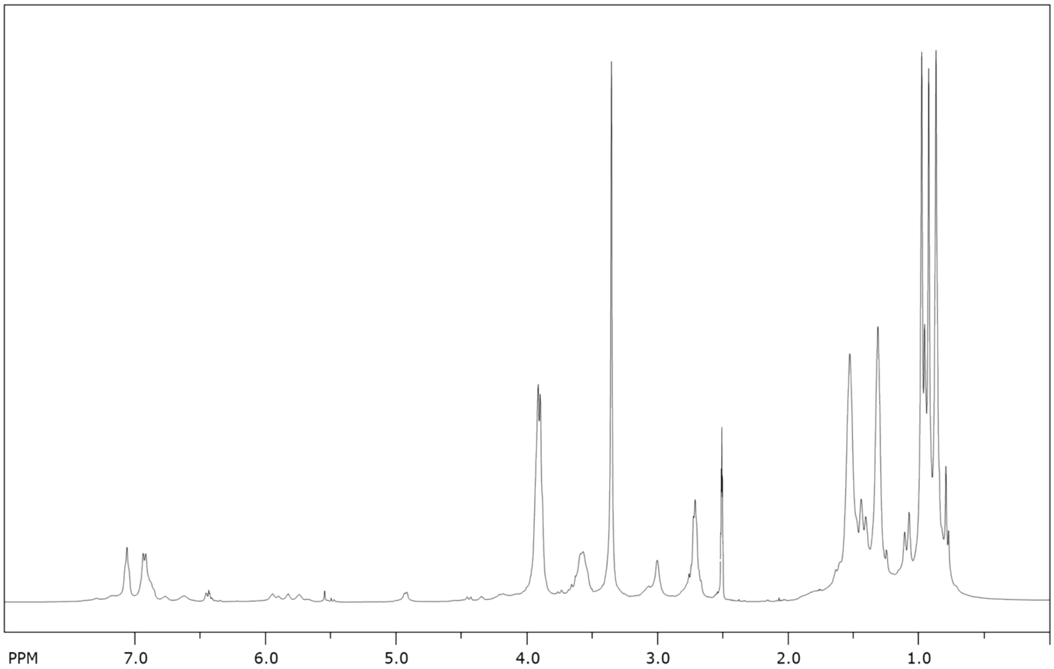

Figure S35. ^1H NMR spectrum of PSU-5.

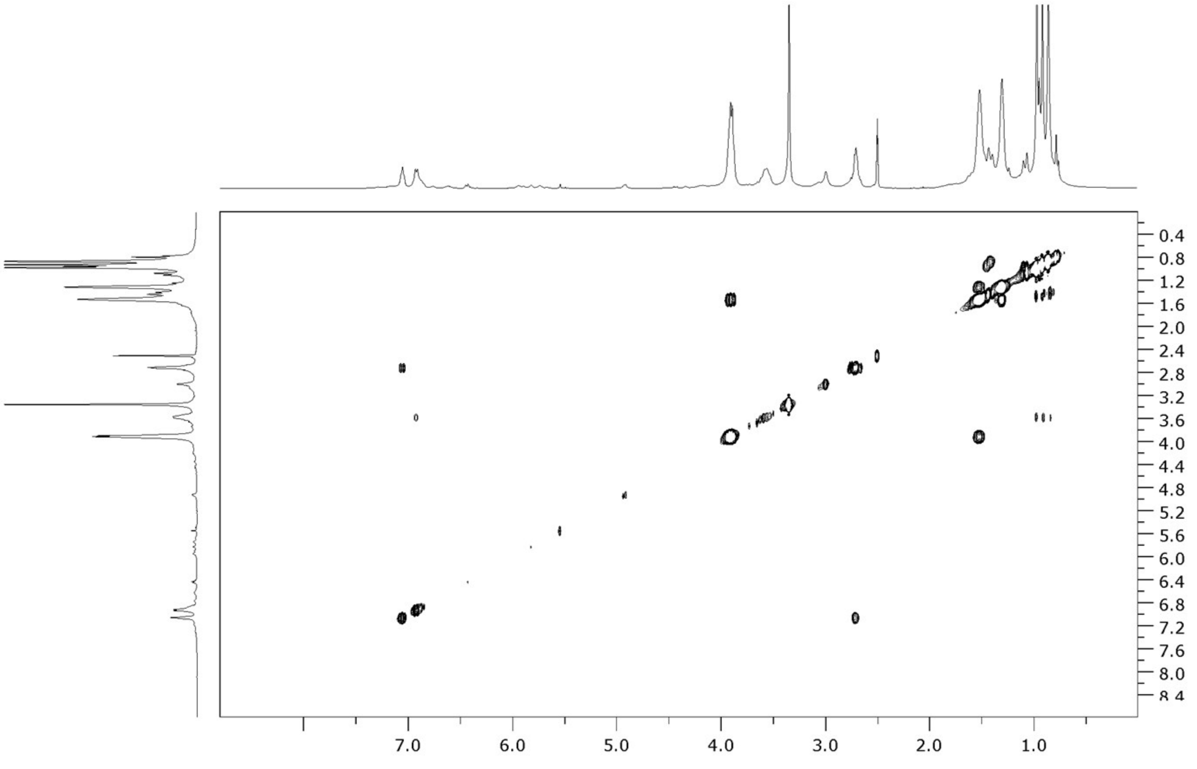

Figure S36. COSY spectrum of PSU-5.

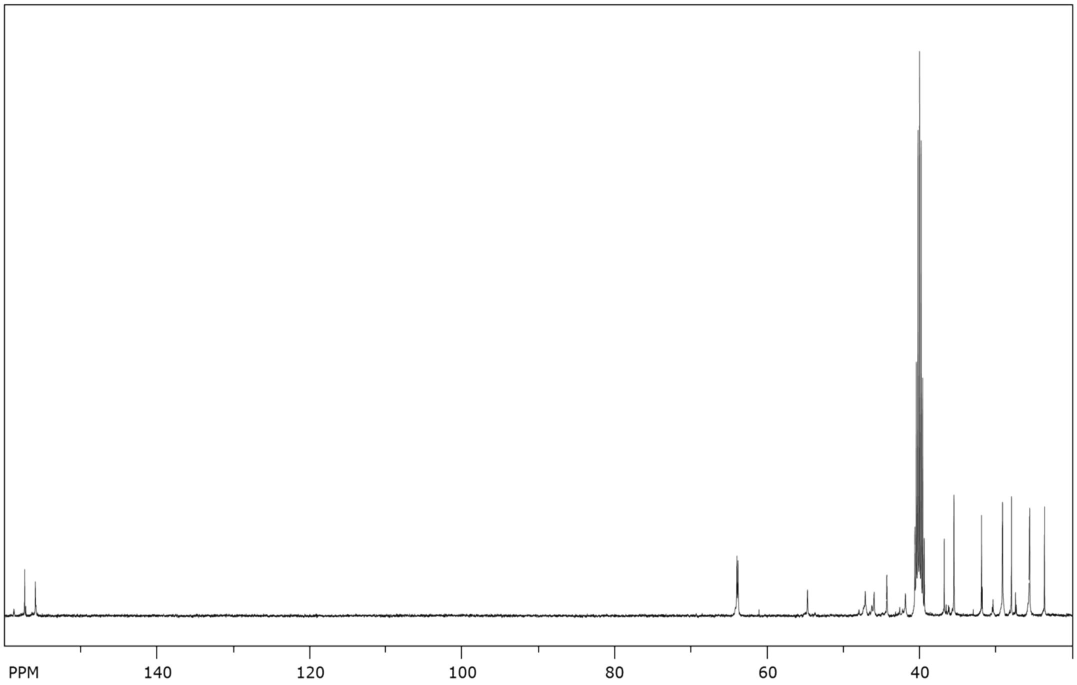

Figure S37. ^{13}C NMR spectrum of PSU-5.

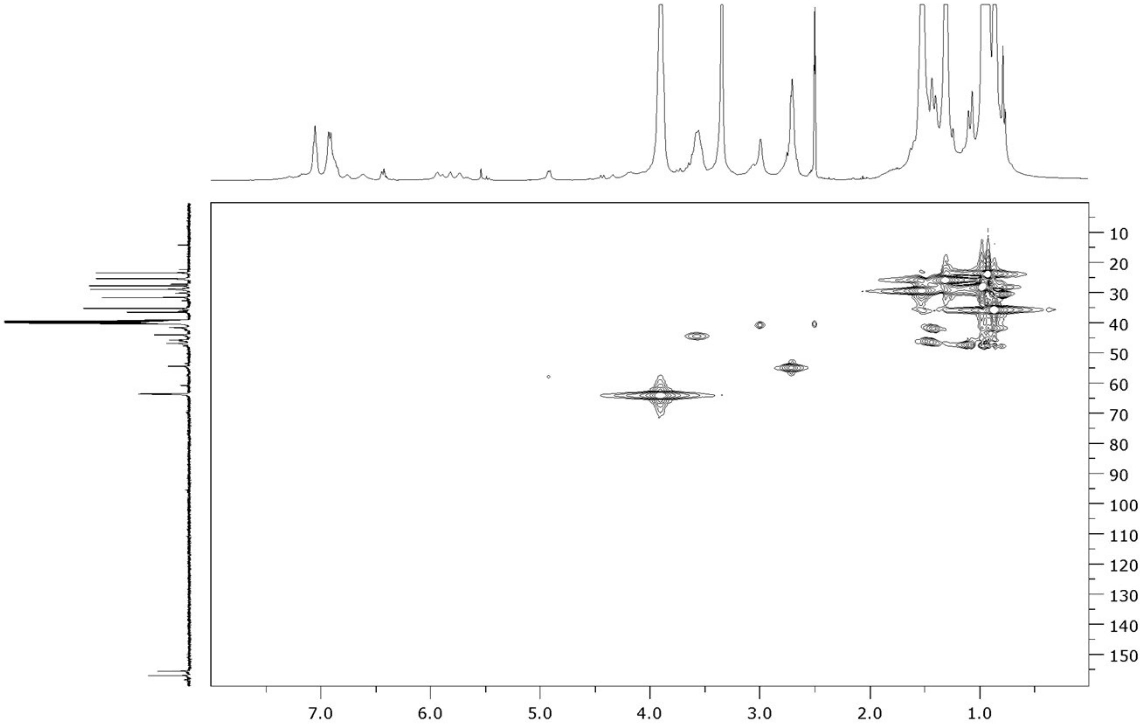

Figure S38. HMQC spectrum of PSU-5.

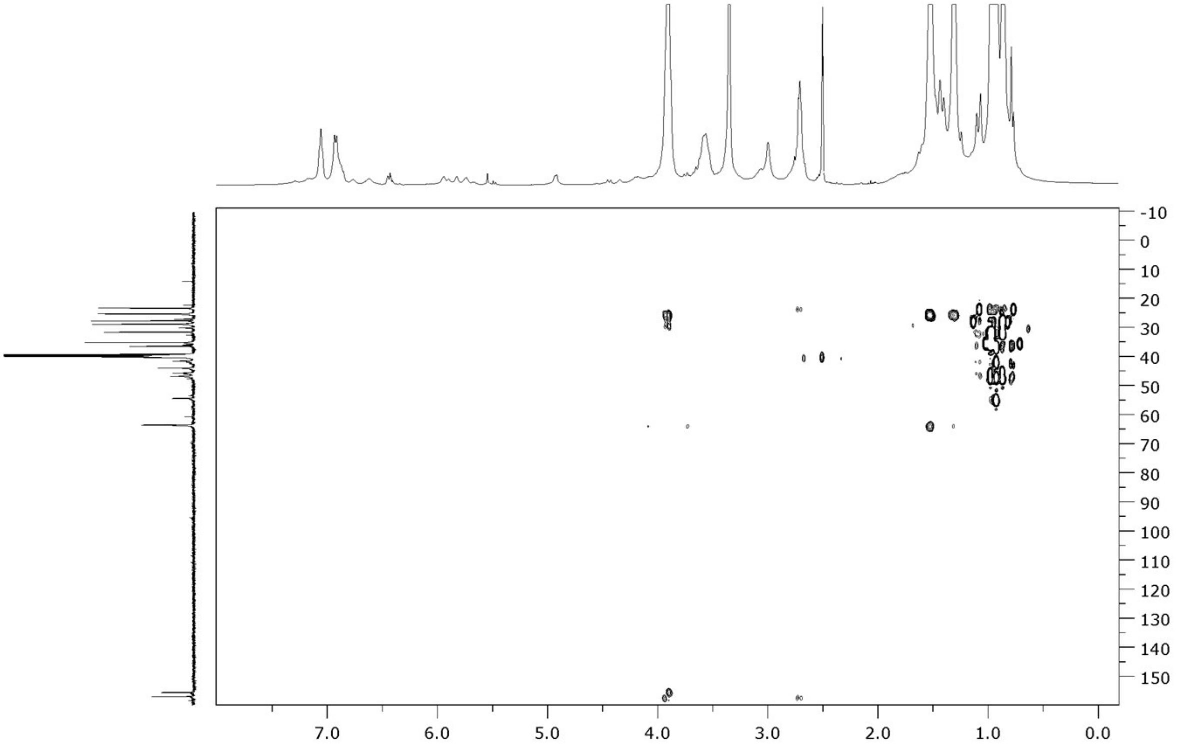

Figure S39. HMBC spectrum of PSU-5.

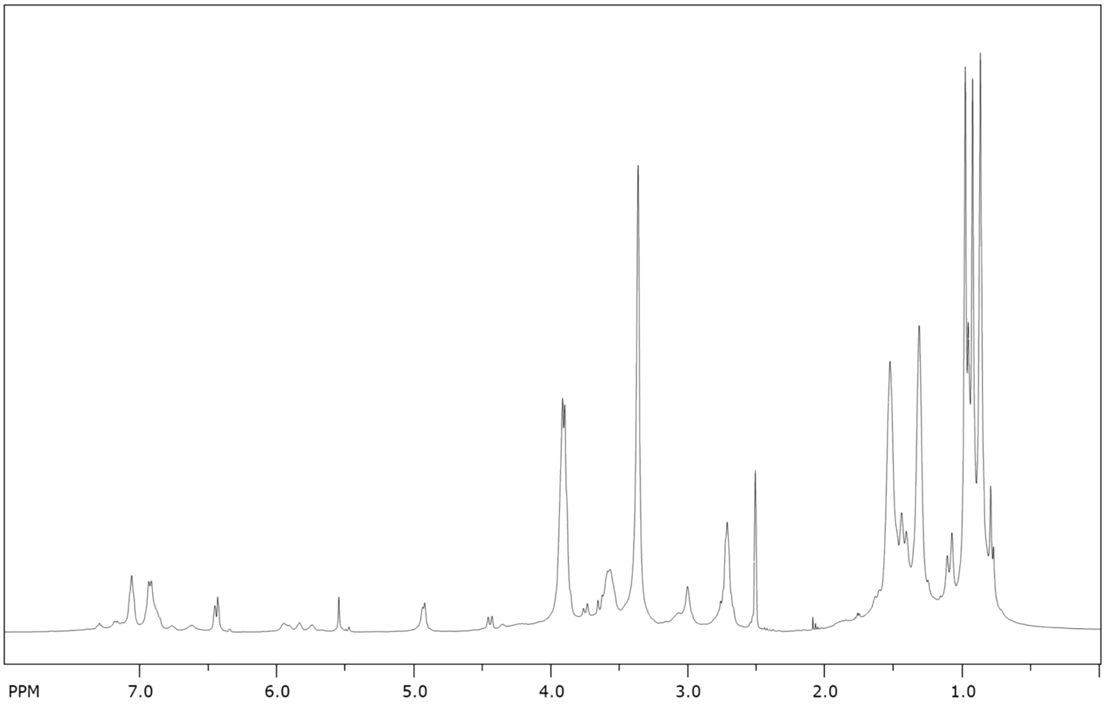

Figure S40. ^{1}H NMR spectrum of PSU-10.

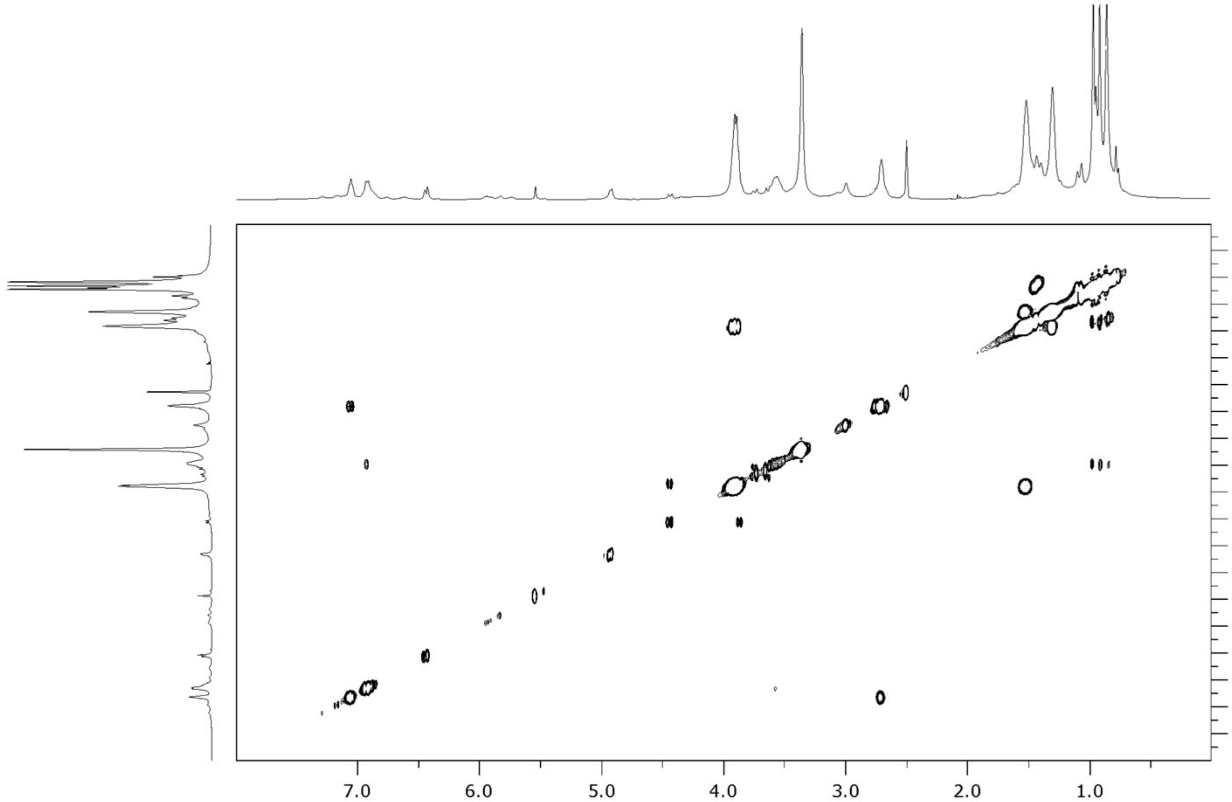

Figure S41. COSY spectrum of PSU-10.

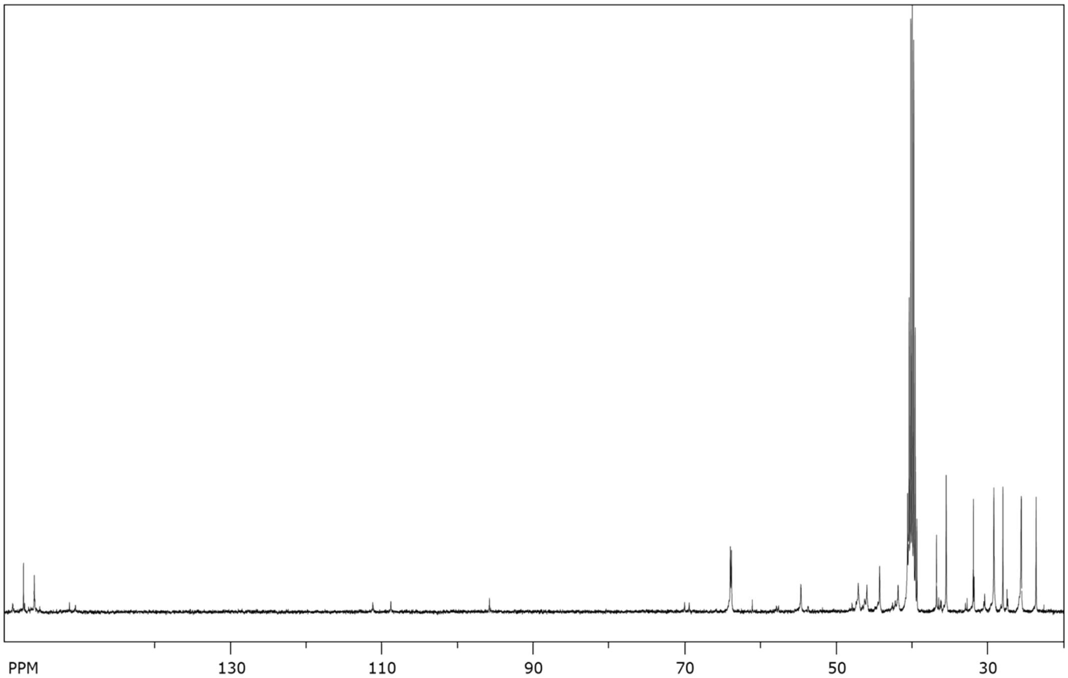

Figure S42. ^{13}C NMR spectrum of PSU-10.

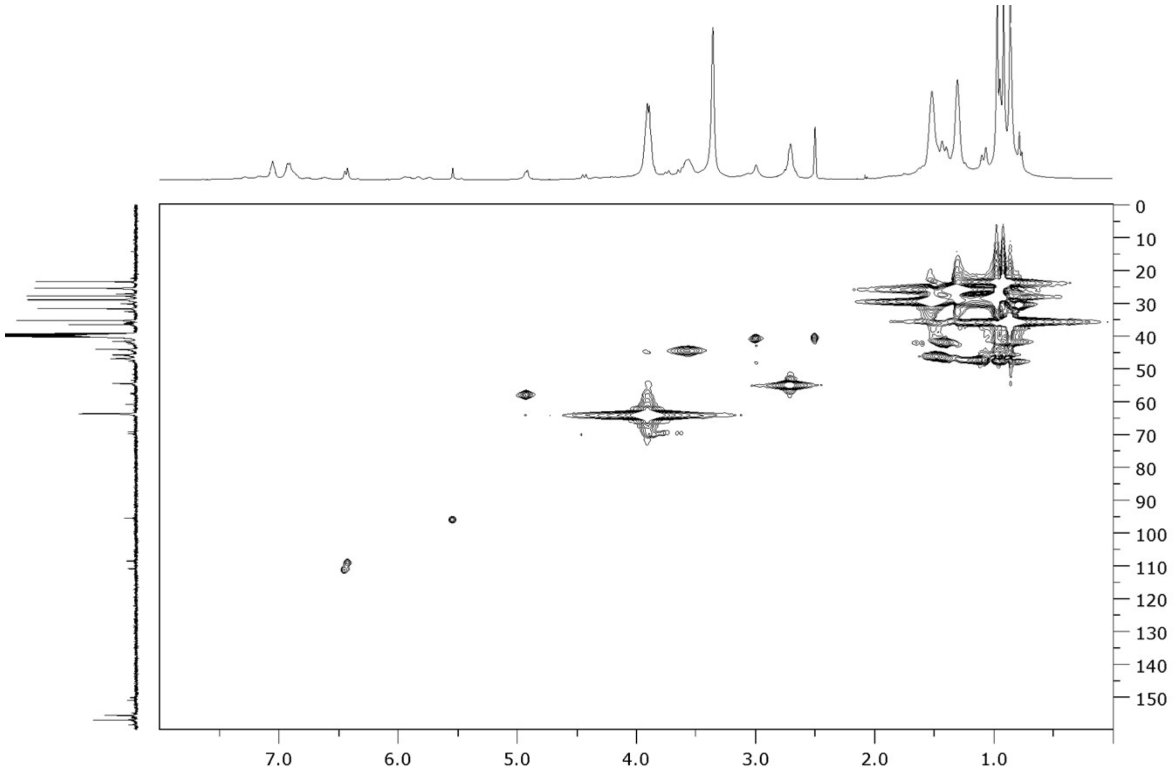

Figure S43. HMQC spectrum of PSU-10.

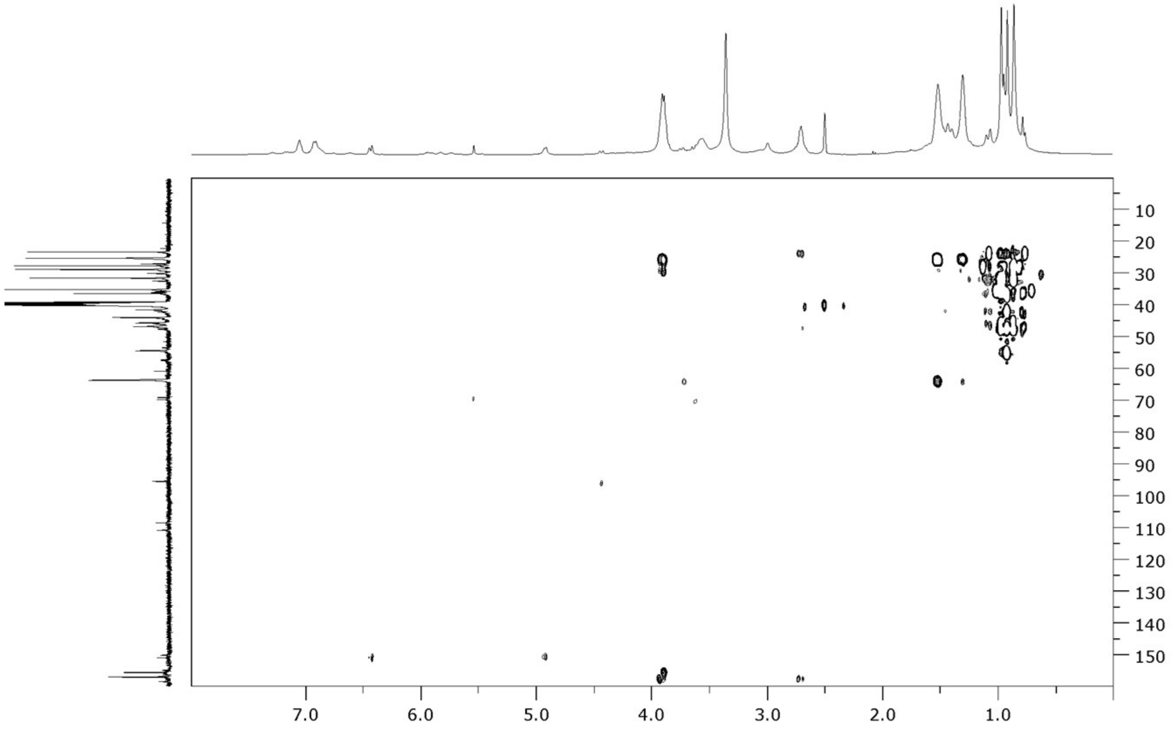

Figure S44. HMBC spectrum of PSU-10.

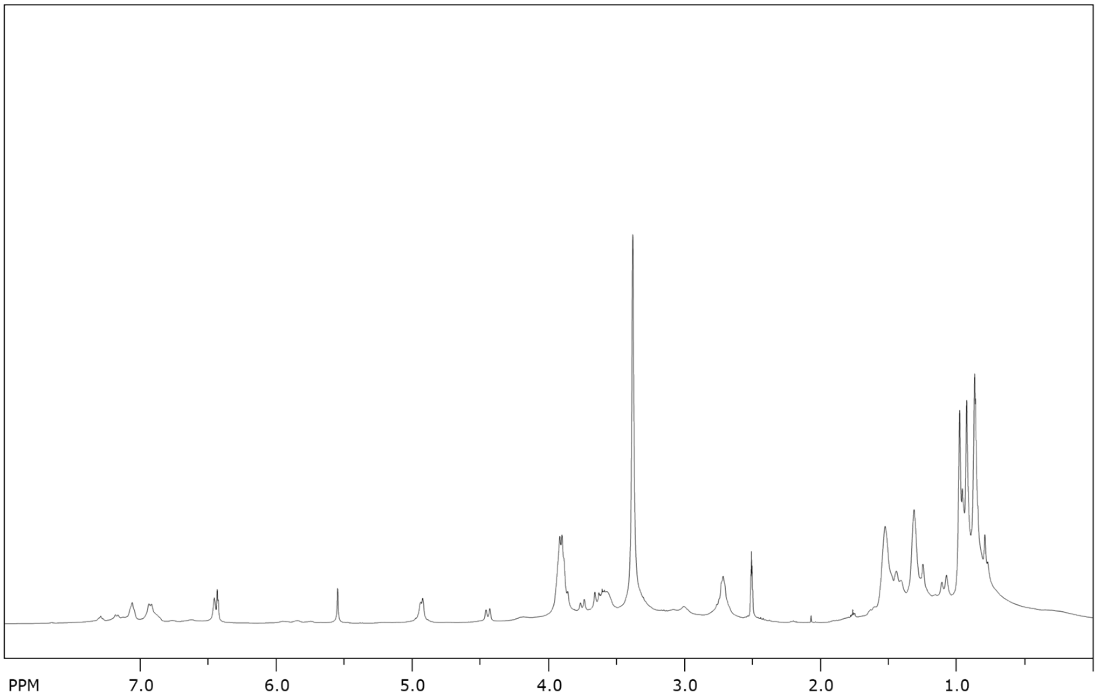

Figure S45. ^{1}H NMR spectrum of PSU-18.

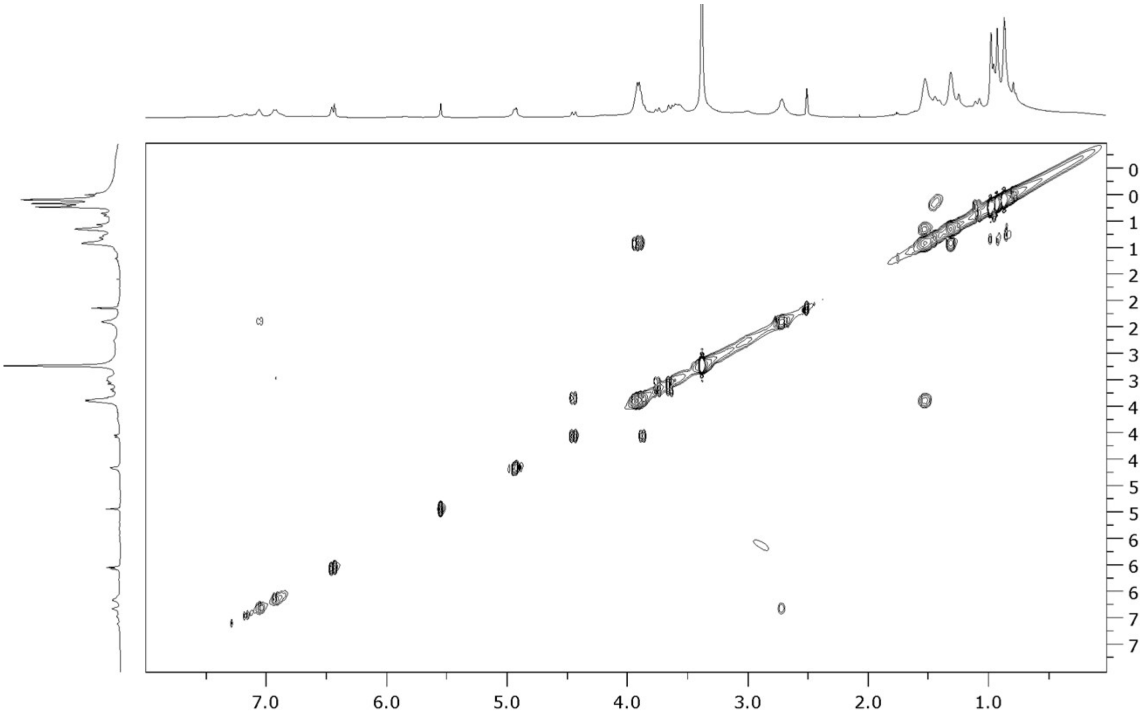

Figure S46. COSY spectrum of PSU-18.

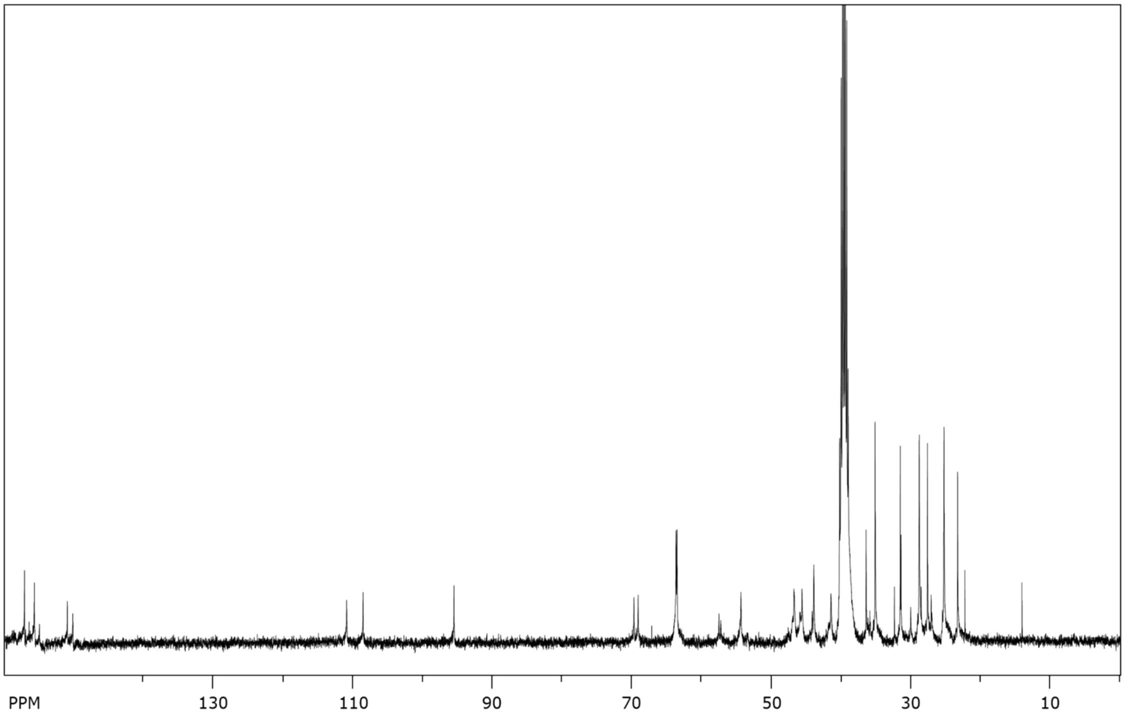

Figure S47. ^{13}C NMR spectrum of PSU-18.

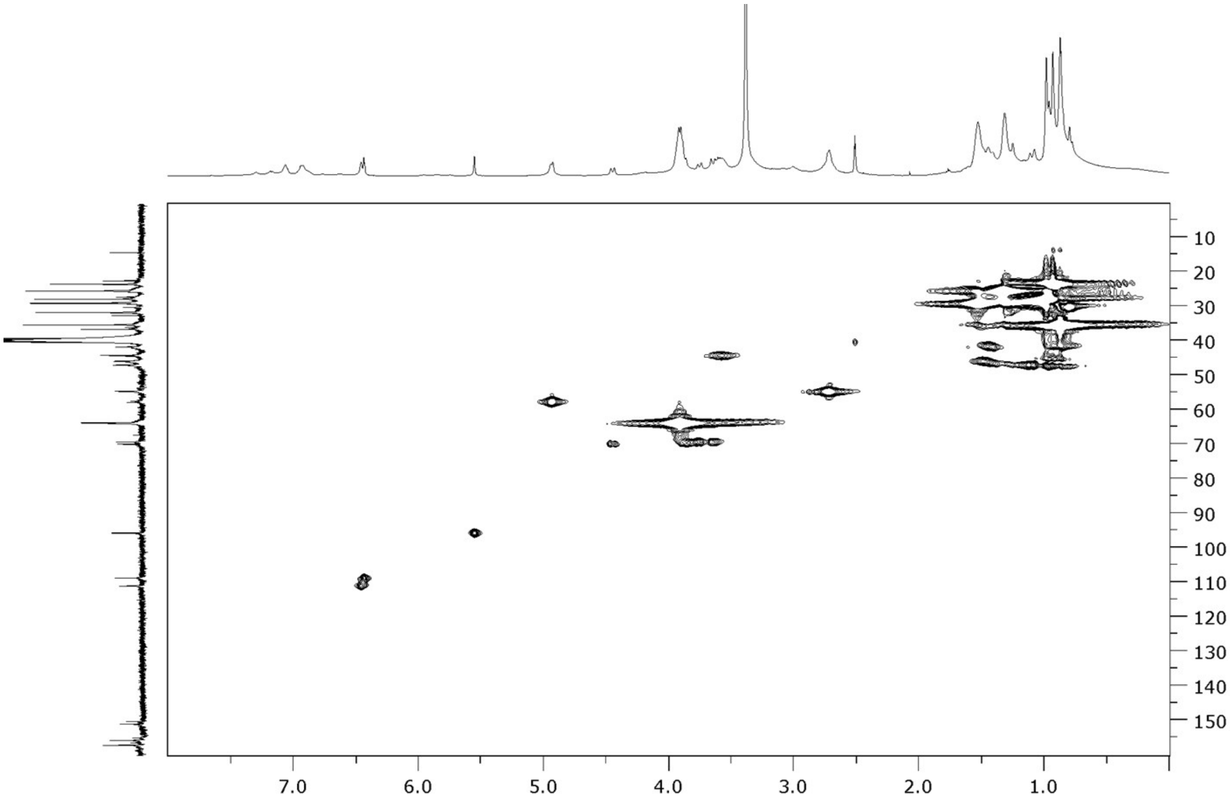

Figure S48. HMQC spectrum of PSU-18.

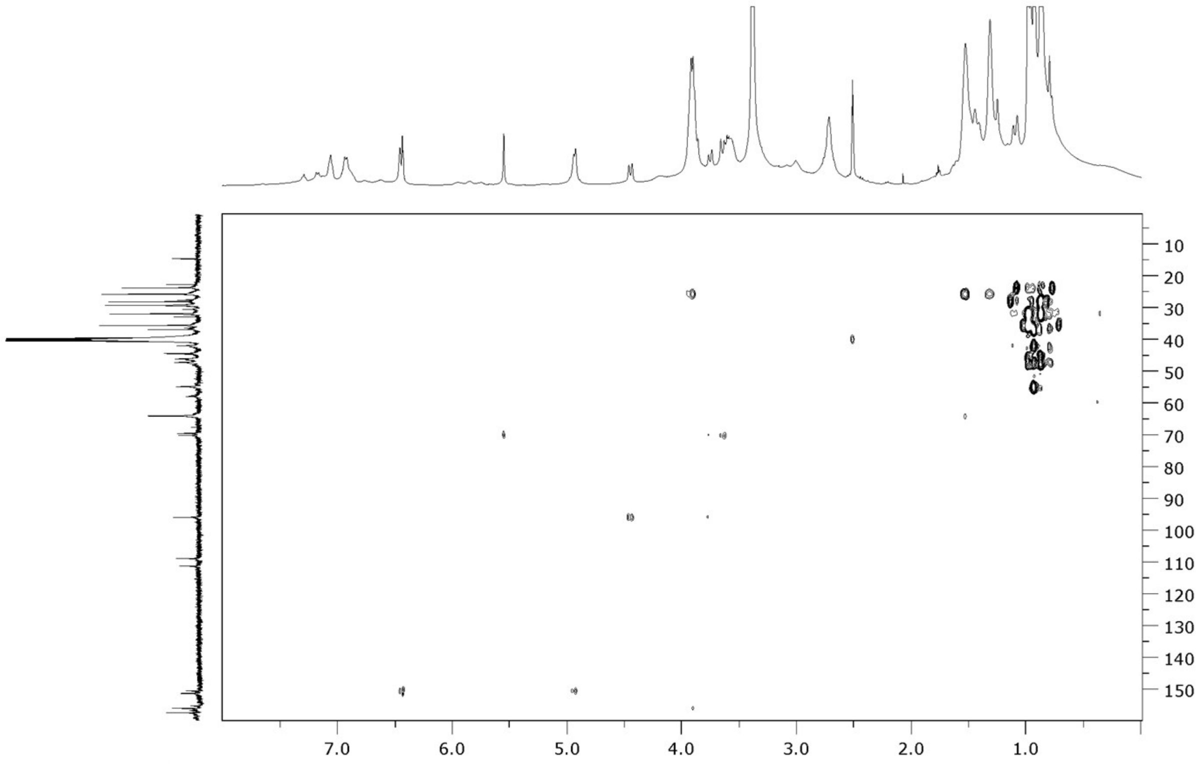

Figure S49. HMBC spectrum of PSU-18

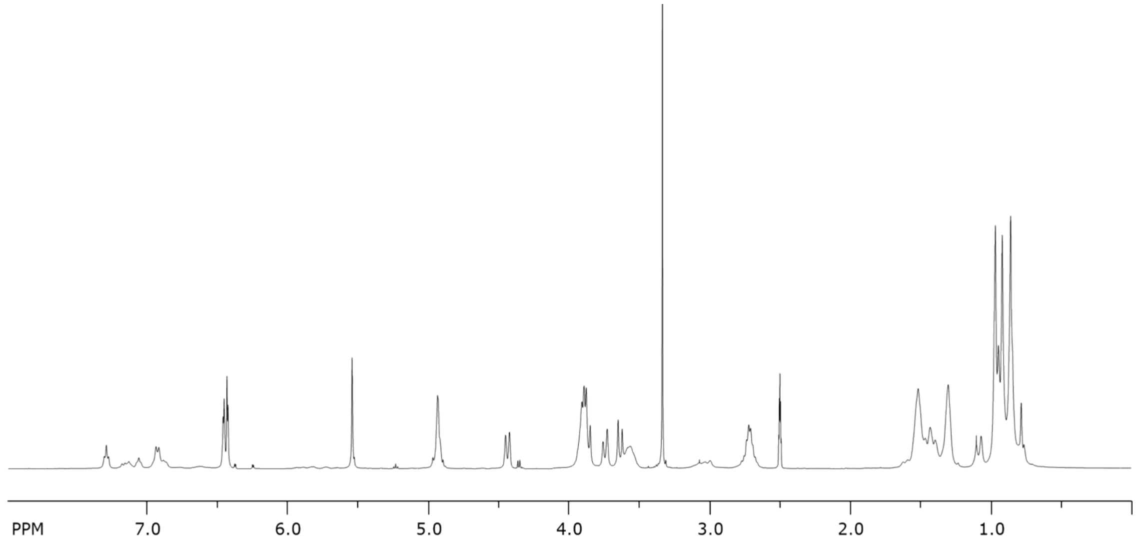

Figure S50. ^{1}H NMR spectrum of PSU-43.

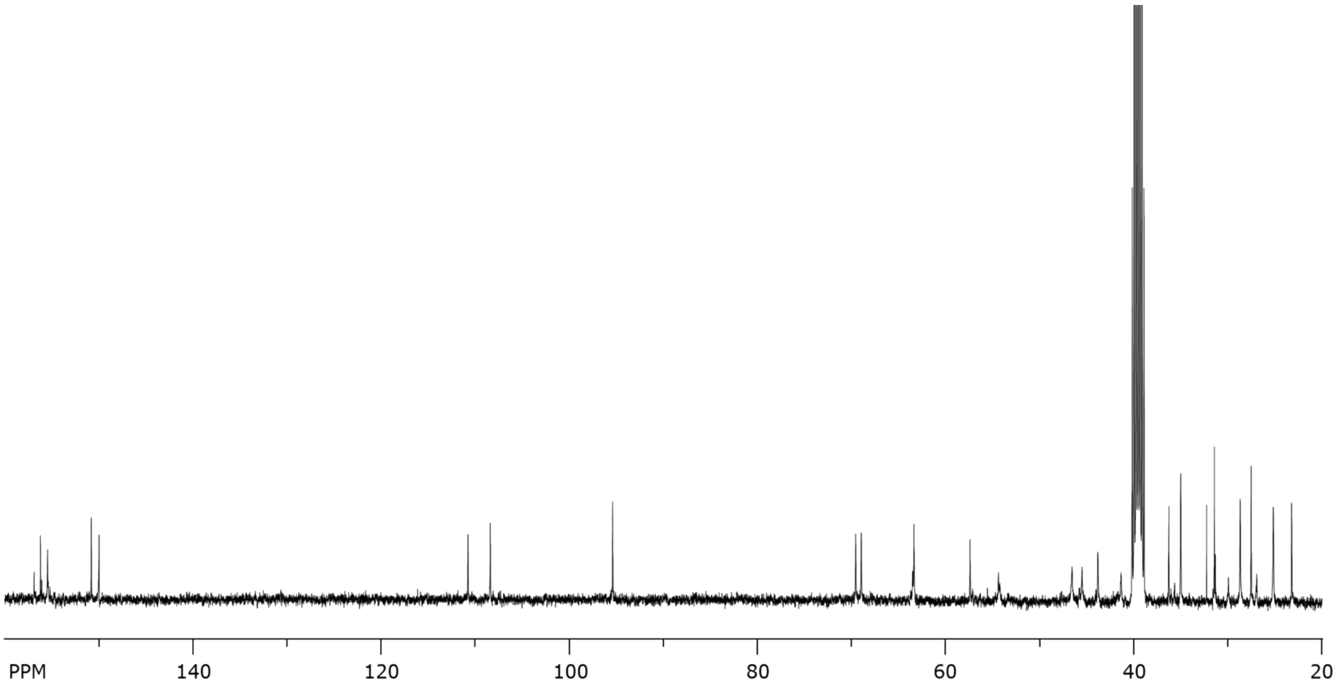

Figure S51. ^{13}C NMR spectrum of PSU-43.

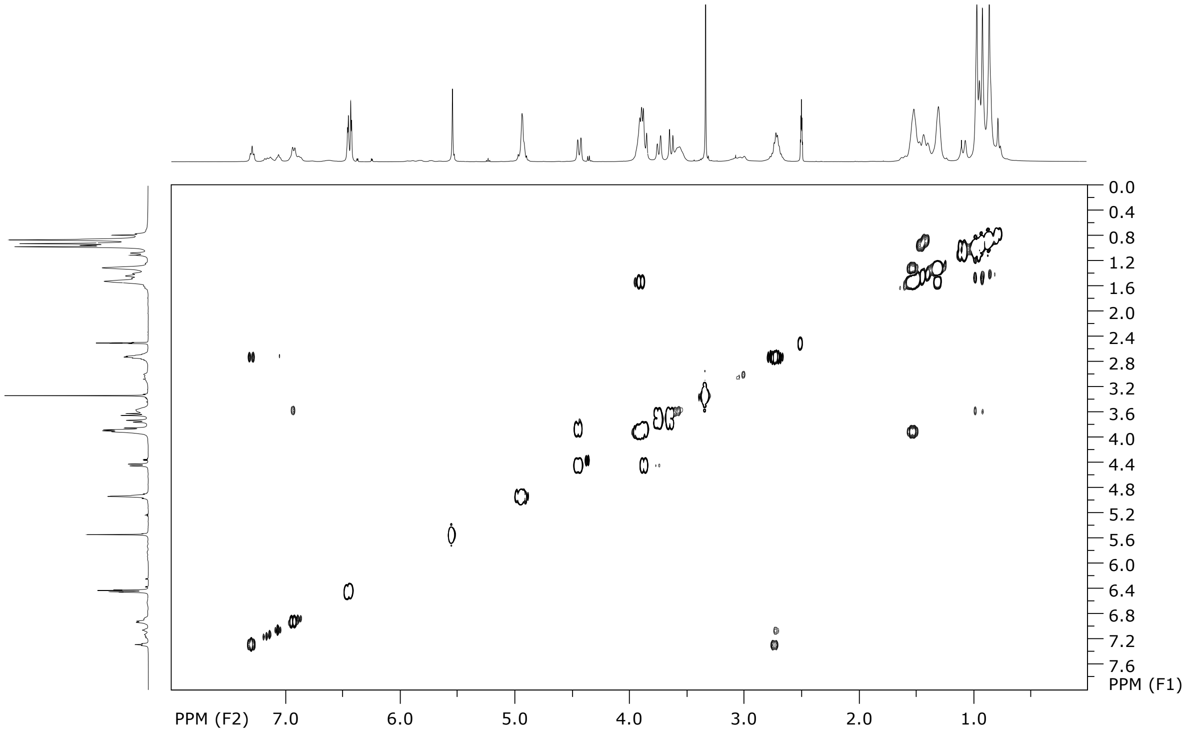

Figure S52. COSY spectrum of PSU-43.

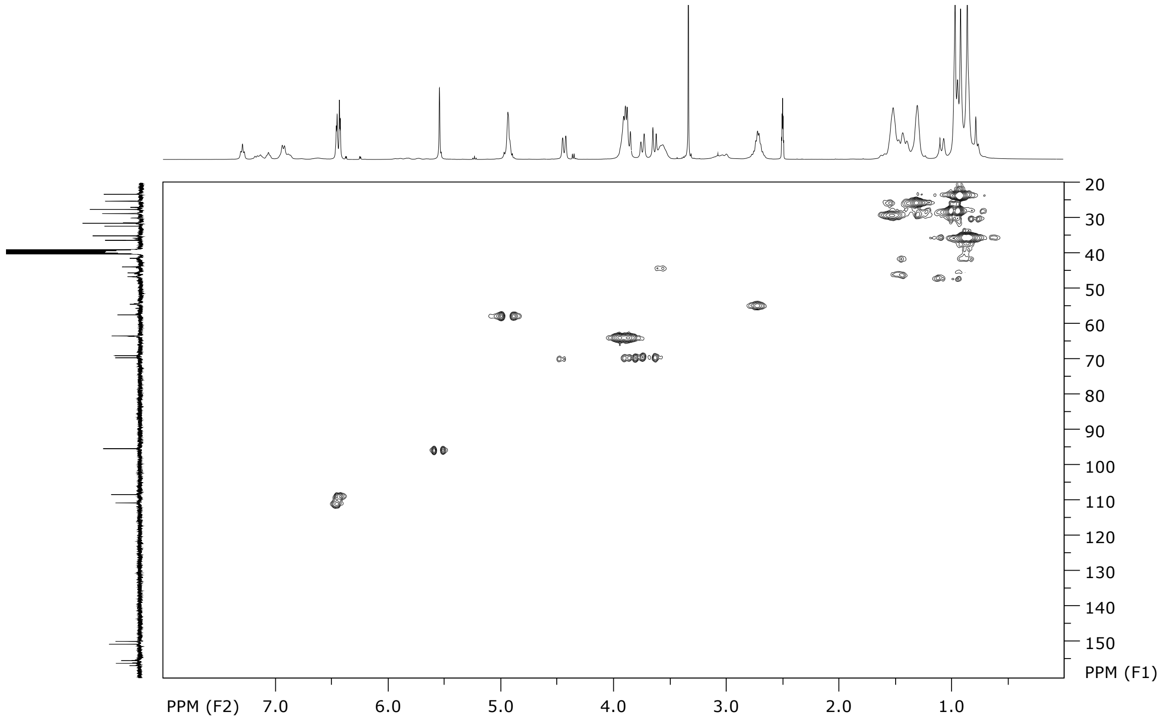

Figure S53. HMQC spectrum of PSU-43.

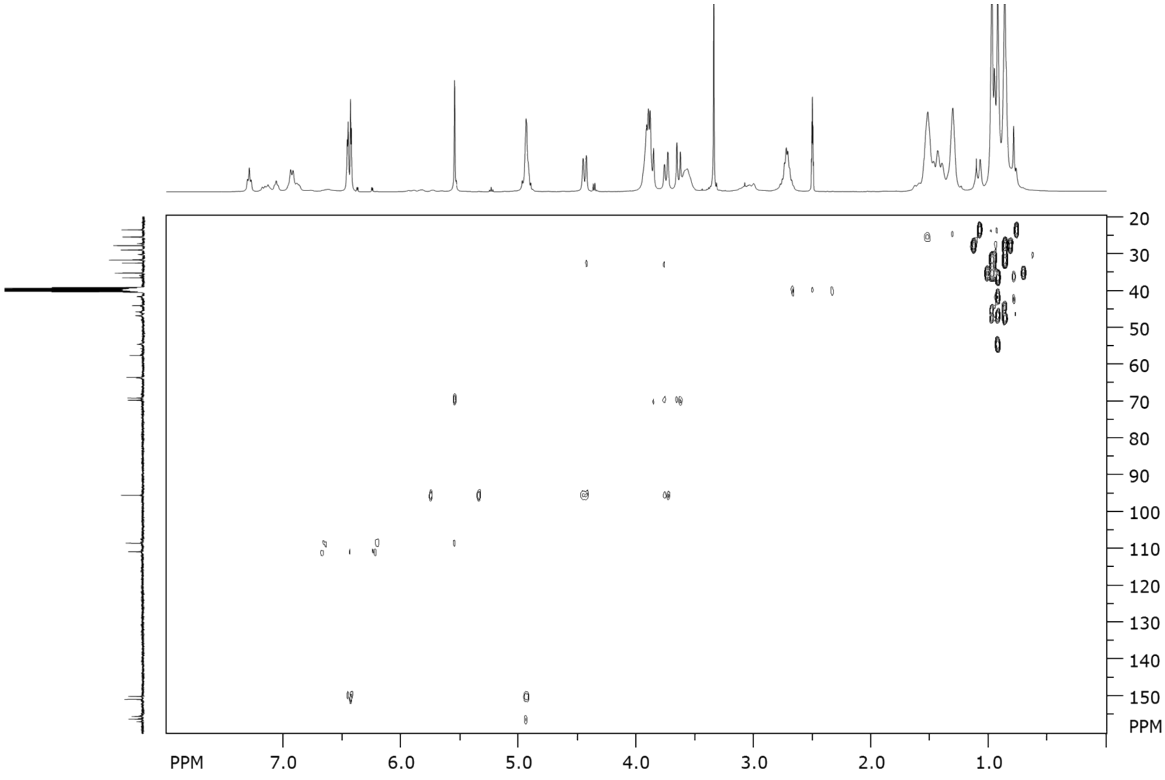

Figure S54. HMBC spectrum of PSU-43

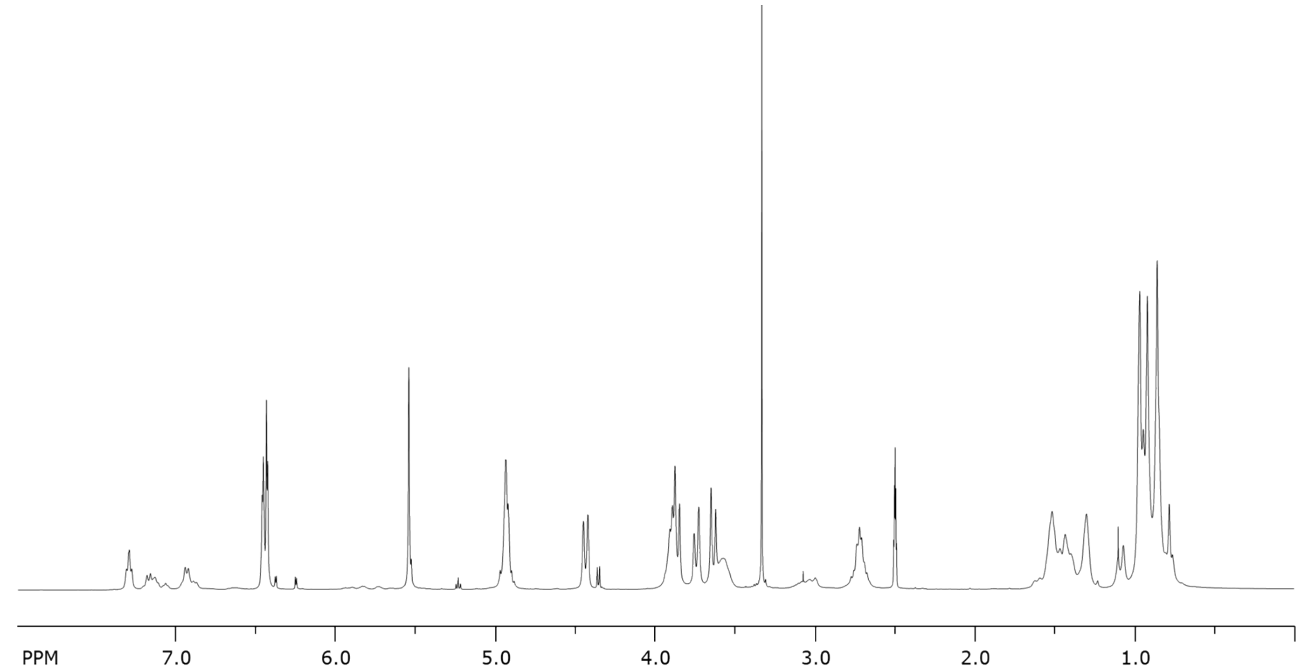

Figure S55. ^{1}H NMR spectrum of PSU-62.

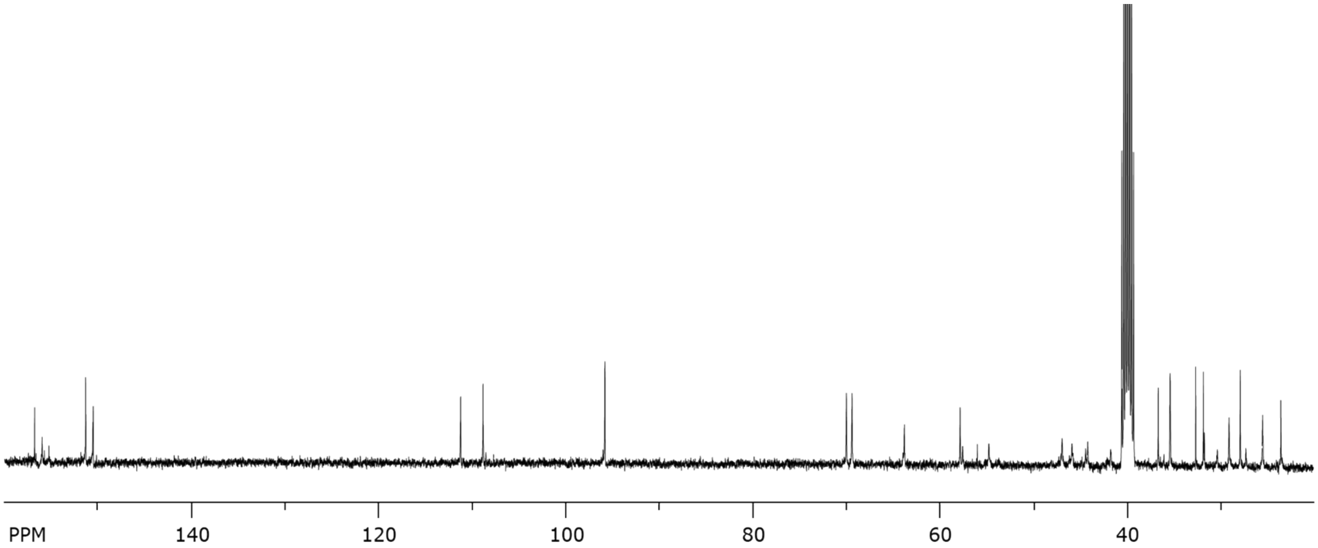

Figure S56. ^{13}C NMR spectrum of PSU-62.

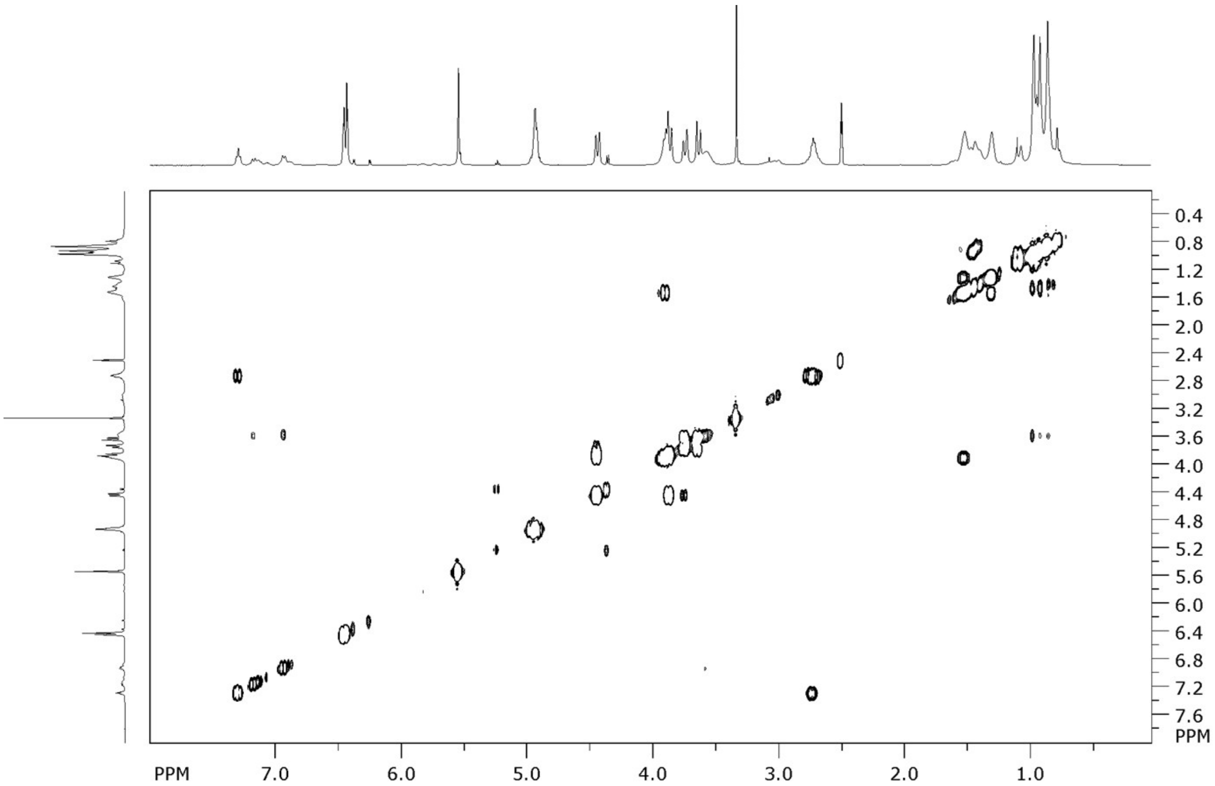

Figure S57. COSY spectrum of PSU-62.

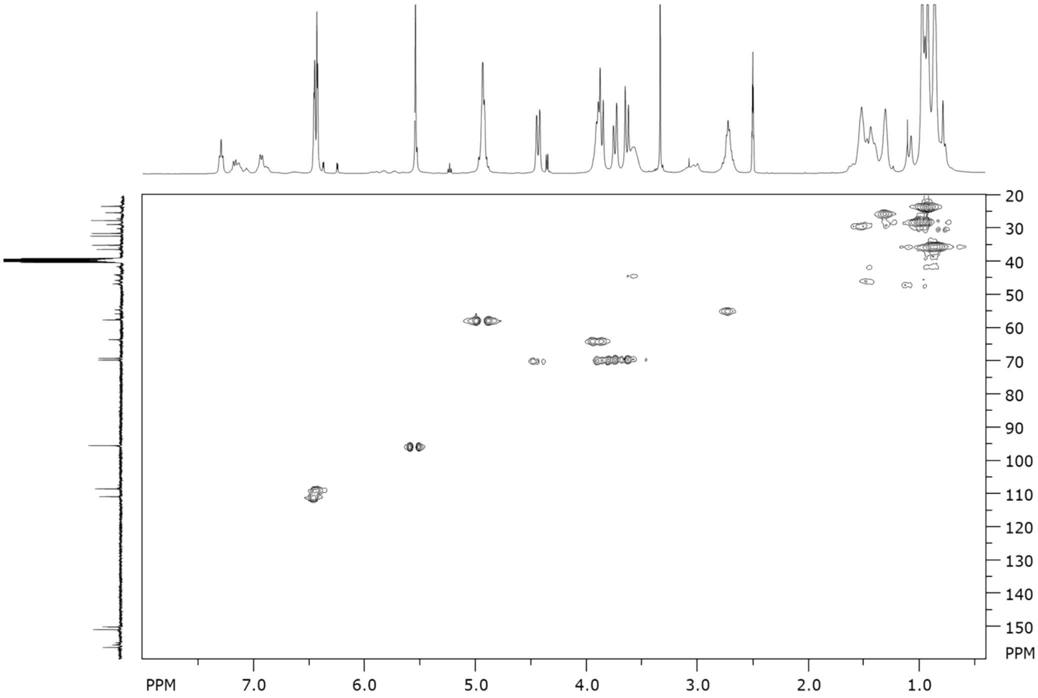

Figure S58. HMQC spectrum of PSU-62.

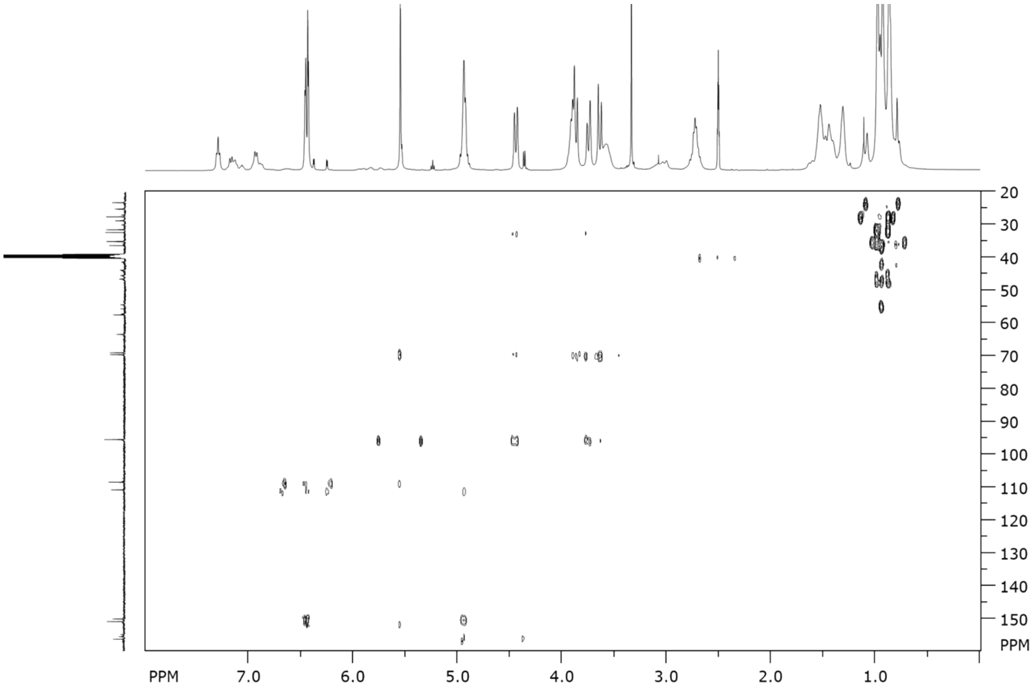

Figure S59. HMBC spectrum of PSU-62.

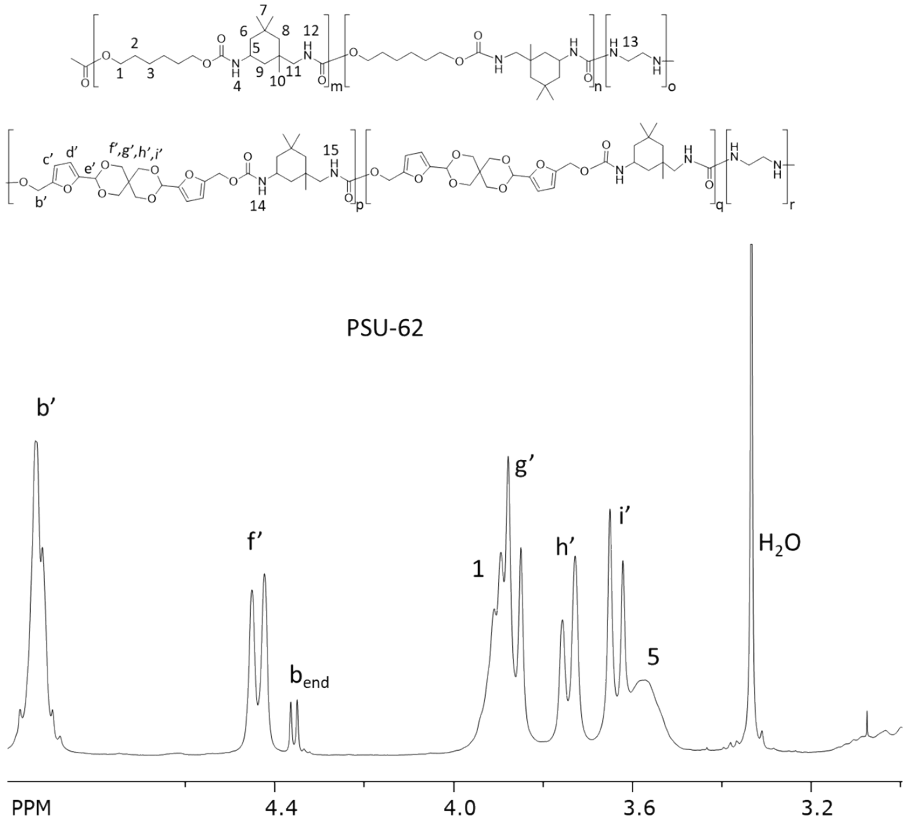

Figure S60. ^{1}H NMR spectrum of PSU-62 (expanded from 5.0 to 3.0 ppm).

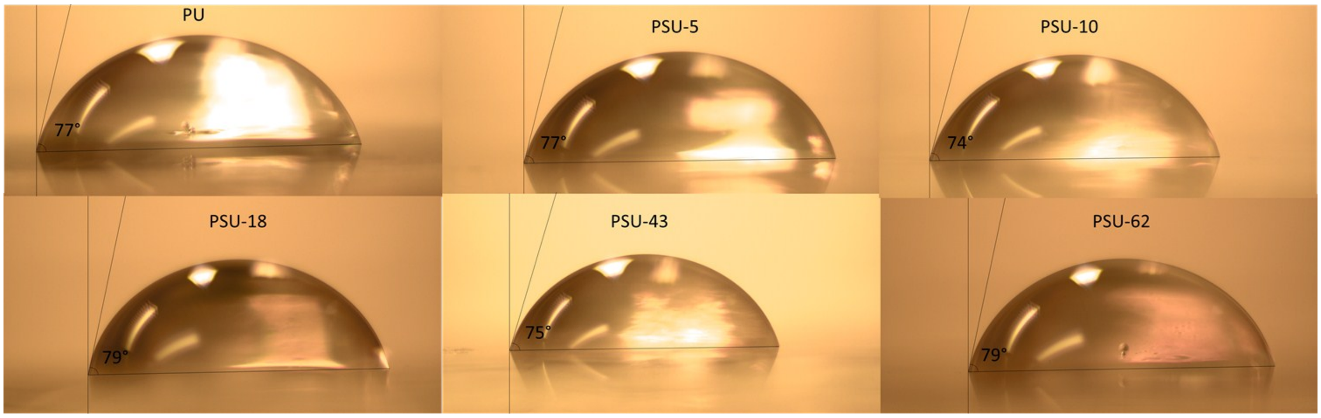

Figure S61. Photograph of a water droplet placed on the different poly(urethane-urea) films.

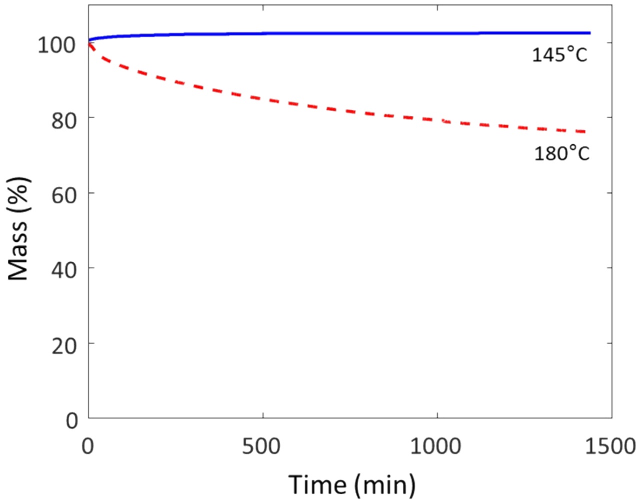

Figure S62. Isothermal thermogram for Monomer **S** at 145 °C and 180 °C.

Calculation of M_n according to the integral of the signals in ^{1}H NMR spectra of polyurethanes:

M_{IPDI} = 222.28 g/mol

M_{HD} = 118.17 g/mol

M_S = 352.34 g/mol

Assume x is the content of Monomer **S** with respect to IPDI, so the averaged molecular weight for the diols, M(average diol), is

M(average diol) = (1-x)*118.17+x*352.34

Then, the molecular weight for an averaged repeating unit of PU (or PSU), M_{RU}, is

M(average diol)+M_{IPDI} = M_{RU}

In the equation above, the contribution from the chain extender (ethylene diamine) is neglected, because it was used with relatively small extend (~10mol%) compared with IPDI.

Furthermore, by assuming that both end groups are the alcohol groups from Monomer **S**, so

DP_n = [Integral for IPDI] / [Integral for end group], where integral of IPDI was obtained by the integral of signal 11 (Fig. 7), and the integral of end group was obtained as the integral of signal a_{end} (Fig. 7).

Finally, the molecular weight of polyurethanes was calculated as $M_n = DP_n*M_{RU}$